

# A universal framework for learning the elliptical mixture model

Shengxi Li, *Student Member, IEEE*, Zeyang Yu, Danilo Mandic, *Fellow, IEEE*

**Abstract**—Mixture modelling using elliptical distributions promises enhanced robustness, flexibility and stability over the widely employed Gaussian mixture model (GMM). However, existing studies based on the elliptical mixture model (EMM) are restricted to several specific types of elliptical probability density functions, which are not supported by general solutions or systematic analysis frameworks; this significantly limits the rigour and the power of EMMs in applications. To this end, we propose a novel general framework for estimating and analysing the EMMs, achieved through Riemannian manifold optimisation. First, we investigate the relationships between Riemannian manifolds and elliptical distributions, and the so established connection between the original manifold and a reformulated one indicates a mismatch between those manifolds, the major cause of failure of the existing optimisation for solving general EMMs. We next propose a universal solver which is based on the optimisation of a re-designed cost and prove the existence of the same optimum as in the original problem; this is achieved in a simple, fast and stable way. We further calculate the influence functions of the EMM as theoretical bounds to quantify robustness to outliers. Comprehensive numerical results demonstrate the ability of the proposed framework to accommodate EMMs with different properties of individual functions in a stable way and with fast convergence speed. Finally, the enhanced robustness and flexibility of the proposed framework over the standard GMM are demonstrated both analytically and through comprehensive simulations.

**Index Terms**—Finite mixture model, elliptical distribution, manifold optimisation, robust estimation, influence function

## I. INTRODUCTION

Finite mixture models have a prominent role in statistical machine learning, owing to their ability to enhance probabilistic awareness in many learning paradigms, including clustering, feature extraction and density estimation [1]. Among such models, the Gaussian mixture model (GMM) is the most widely used, with its stemming popularity from a simple formulation and the conjugate property of Gaussian distribution. Despite mathematical elegance, a standard GMM estimator is subject to robustness issues, as even a slight deviation from the Gaussian assumption or a single outlier in data can significantly degrade the performance or even break down the estimator [2]. Another issue with GMMs is their limited flexibility, which limits their application for rapidly emerging multi-faceted data which are almost invariably unbalanced; sources of such imbalance may be due to different natures of the data channels involved, different powers in the constitutive channels, or temporal misalignment [3].

An important class of flexible multivariate analysis techniques are elliptical distributions, which are quite general and include as special cases a range of standard distributions, such as the Gaussian distribution, the logistic distribution and the  $t$ -distribution [4]. The desired robustness to unbalanced multichannel data is naturally catered for elliptical distributions; indeed estimating certain elliptical distribution types results in robust M-estimators [5], thus making them a natural candidate for robust and flexible mixture modelling. It is therefore natural to consider mixtures of elliptical distributions, or elliptical mixture model (EMM), in probabilistic modelling ways. By virtue of EMMs, it is possible to select a wide range of standard distributions as EMM components to exhibit different properties, which makes EMMs both more flexible in capturing intrinsic structures and more meaningful in interpreting data, as compared to the GMM. Another appealing property of EMMs is their identifiability in mixture problems, which has been proved by Holzmann *et al.* [6]. In addition, it has been reported that several members of the EMMs can also effectively mitigate the singular covariance problem experienced in the GMM [7].

Existing mixture models related to elliptical distributions are most frequently based on the  $t$ -distribution [7], [8], [9], the Laplace distribution [10], or the hyperbolic distribution [11]; these are optimised by a specific generalised expectation-maximisation process, called the iteratively reweighting algorithm (IRA) [12]. These elliptical distributions belong to the class of *scale mixture of normals* [13], where the IRA actually operates as an expectation maximisation (EM) algorithm, and such an EMM model is guaranteed to converge. However, for other types of elliptical distributions, the convergence of the IRA requires constraints on both the type of elliptical distributions and the data structure [12], [14], [15]. Therefore, although beneficial and promising, the development of a universal method for estimating the EMM is non-trivial, owing to both theoretical and practical difficulties.

To this end, this work sets out to rigorously establish a whole new framework for estimating and analysing the identifiable EMMs, thus opening an avenue for practical approaches based on general EMMs. More specifically, we first analyse the second-order statistical differential tensors to obtain the Riemannian metrics on the mean and the covariance of elliptical distributions. A reformulation trick is typically used to convert the mean-covariance-estimation problem into a covariance-estimation-only problem [12]. We further investigate the relationship between the manifolds with and without the reformulation, and find that an equivalence of

Shengxi Li, Zeyang Yu and Danilo Mandic are with the department of Electrical and Electronic of Imperial College London.

the two manifolds only holds in the Gaussian case. since for general elliptical distributions, the equivalence is not guaranteed, this means that a direct optimisation on the reformulated manifold cannot yield the optimum for all EMMs. To overcome this issue, we propose a novel method with a modified cost of EMMs and optimise it on a matched Riemannian manifold via manifold gradient descent, where the same optimum as in the original problem is achieved in a fast and stable manner. The corresponding development of a gradient-based solver, rather than the EM-type solver (i.e., the IRA), is shown to be beneficial, as it offers more flexibility in model design, through various components and regularisations. We should point out that even for the EMMs where the IRA converges, our proposed method still outperforms the widely employed IRA. We finally systematically verify the robustness of EMMs by proving the influence functions (IFs) in closed-form, which serves as the theoretical bound.

The recent related work in [16], [17] adopts manifold optimisation for GMM problems by simply optimising on the intrinsic manifold. However, this strategy is inadequate in EMM problems due to a mismatch in manifolds for optimisation, which leads to a different optimum after reformulation. More importantly, as the flexibility of EMMs allows for inclusion of a wide range of distributions, this in turn regimes the statistics of mixture modelling to be considered in the optimisation, whilst the work [16], [17] only starts from a manifold optimisation perspective. The key contributions of this work are summarised as follows:

- 1) We justify the usage of Riemannian metrics from the statistics of elliptical distributions, and in this way connect the original manifold with the reformulated one, where the convergence can be highly accelerated.
- 2) We propose a novel method for accurately solving general EMMs in a fast and stable manner, thus making the flexible EMM truly practically applicable.
- 3) We rigorously prove the IFs in closed-form as theoretical bounds to qualify the robustness of EMMs, thus providing a systematic framework for treating the flexibility of EMMs.

## II. PRELIMINARIES AND RELATED WORKS

As our initiative is to solve the EMMs from the perspective of manifold optimisation, we first provide the preliminaries on the manifold related to probability distributions in Section II-A. Then, we introduce the preliminaries and notations of the elliptical distributions in Section II-B. We finally review the related EMM works in Section II-C.

### A. Preliminaries on the Riemannian manifold

A Riemannian manifold  $(\mathcal{M}, \rho)$  is a smooth (differential) manifold  $\mathcal{M}$  (i.e., locally homeomorphic to the Euclidean space) which is equipped with a smoothly varying inner product  $\rho$  on its tangent space. The inner product also defines a Riemannian metric on the tangent space, so that the length of a curve and the angle between two vectors can be correspondingly defined. Curves on the manifold with the shortest paths are called *geodesics*, which exhibit

constant instantaneous speed and generalise straight lines in the Euclidean space. The distance between two points on  $\mathcal{M}$  is defined as the minimum length of all geodesics connecting these two points.

We shall use the symbol  $T_{\Sigma}\mathcal{M}$  to denote the *tangent space* at the point  $\Sigma$ , which is the first-order approximation of  $\mathcal{M}$  at  $\Sigma$ . Consequently, the *Riemannian gradient* of a function  $f$  is defined with regard to the equivalence between its inner product with an arbitrary vector  $\xi$  on  $T_{\Sigma}\mathcal{M}$  and the Fréchet derivative of  $f$  at  $\xi$ . Moreover, a smooth mapping from  $T_{\Sigma}\mathcal{M}$  and  $\mathcal{M}$  is called the *retraction*, whereby an exponential mapping obtains the point on geodesics in the direction of the tangent space. Because the tangent spaces vary across different points on  $\mathcal{M}$ , *parallel transport* across different tangent spaces can be introduced on the basis of the Levi-Civita connection, which preserves the inner product and the norm. Then, we can convert a complex optimisation problem on  $\mathcal{M}$  into a more analysis friendly space, that is,  $T_{\Sigma}\mathcal{M}$ . For a comprehensive text on the optimisation on the Riemannian manifold, we refer to [18]. Therefore, on the basis of the above basic operations, the manifold optimisation can be performed by the Riemannian gradient descent [19]. The retraction is then utilised to map a step descent from the tangent space to the manifold. To accelerate gradient descent optimisation, the parallel transport can be utilised to accumulate the first-order moments [20], [21], [22], [23], [24].

When restricted to the manifold of positive definite matrices, it is natural to define the manifold via the statistics of Gaussian distributions because the covariance of the Gaussian distribution intrinsically satisfies the positive definiteness property. Pioneering in this direction is the work of Rao, which introduced the Rao distance to define the statistical difference between two multivariate Gaussian distributions [25]. This distance was later generalised and calculated in closed-form by [26], [27], [28], to obtain an explicit metric (also called the Fisher-Rao metric) is obtained. However, with regard to other distributions, the corresponding Fisher-Rao metric is not guaranteed to be well suited for optimisation [29].

### B. Preliminaries on the elliptical distributions

A random variable  $\mathcal{X} \in \mathbb{R}^M$  is said to have an elliptical distribution if and only if it admits the following stochastic representation [30],

$$\mathcal{X} \stackrel{d}{=} \boldsymbol{\mu} + \mathcal{R}\boldsymbol{\Lambda}\mathcal{U}, \quad (1)$$

where  $\mathcal{R} \in \mathbb{R}^+$  is a non-negative real scalar random variable which models the tail properties of the elliptical distribution;  $\mathcal{U} \in \mathbb{R}^{M'}$  is a random vector that is uniformly distributed on a unit spherical surface with the probability density function (pdf) within the class of  $\Gamma(M/2)/(2\pi^{M/2})$ ;  $\boldsymbol{\mu} \in \mathbb{R}^M$  is a mean (location) vector, while  $\boldsymbol{\Lambda} \in \mathbb{R}^{M \times M'}$  is a matrix that transforms  $\mathcal{U}$  from a sphere to an ellipse, and the symbol “ $\stackrel{d}{=}$ ” designates “the same distribution”. For a comprehensive review, we refer to [4], [31].

Note that an elliptical distribution does not necessarily possess an explicit pdf, but can always be formulated by its

characteristic function. However, when  $M' = M$ , that is, for a non-singular scatter matrix  $\Sigma = \Lambda\Lambda^T$ , the pdf for elliptical distributions does exist and has the following form

$$p_{\mathcal{X}}(\mathbf{x}) = \det(\Sigma)^{-1/2} \cdot c_M \cdot g(\mathbf{x} - \boldsymbol{\mu})^T \Sigma^{-1} (\mathbf{x} - \boldsymbol{\mu}), \quad (2)$$

where the term  $c_M = \frac{\Gamma(M/2)}{2^M \pi^{M/2}}$  serves as a normalisation term and solely relates to  $M$ . We also denote the Mahalanobis distance  $(\mathbf{x} - \boldsymbol{\mu})^T \Sigma^{-1} (\mathbf{x} - \boldsymbol{\mu})$  by the symbol  $t$  for simplicity. Then, the density generator,  $g(\cdot)$ , can be explicitly expressed as  $t^{-(M-1)/2} p_{\mathcal{R}}(\sqrt{t})$ , where  $t > 0$  and  $p_{\mathcal{R}}(t)$  denotes the pdf of  $\mathcal{R}$ . For example, when  $\mathcal{R} = \chi_M^2$ , where  $\chi_M^2$  denotes the chi-squared distribution of dimension  $M$ ,  $g(t)$  in (2) is then proportional to  $\exp(-t/2)$ , which formulates the multivariate Gaussian distribution. For simplicity, the elliptical distribution in (2) will be denoted by  $\mathcal{E}(\mathbf{x}|\boldsymbol{\mu}, \Sigma, g)$ . We also need to point out that typical EMMs are identifiable [6], which is important in order to uniquely estimate mixture models.

**Remark.** Before proceeding to introduce our work, we shall emphasise the importance of the stochastic representation of (1) in analysing elliptical distributions. Some remarks are as follows:

1) Since  $\mathcal{R}$  is independent of  $\mathcal{U}$ , the Mahalanobis distance  $(\mathbf{x} - \boldsymbol{\mu})^T \Sigma^{-1} (\mathbf{x} - \boldsymbol{\mu})$  ( $=^d \mathcal{R}^2$ ) is thus independent of the normalised random variable  $\Sigma^{-1/2}(\mathbf{x} - \boldsymbol{\mu}) / \sqrt{(\mathbf{x} - \boldsymbol{\mu})^T \Sigma^{-1} (\mathbf{x} - \boldsymbol{\mu})}$  ( $=^d \mathcal{U}$ ), which is an important property in many proofs in this paper.

2) The stochastic representation provides an extremely simple way to generate samples, because only two random variables, i.e., the one-dimensional  $\mathcal{R}$  and uniform  $\mathcal{U}$ , can be easily generated.

3) When  $\mathcal{R}$  is composed from a scale mixture of normal distributions, the IRA method converges [32]. For a general EMM, however, the convergence is not ensured.

### C. Related works on EMMs

The GMM based estimation is well established in the machine learning community. Since our focus is on the EMM, we omit the review of GMM and the readers are referred to [33] for a comprehensive review. To robustify the mixture model, the mixtures of the  $t$ -distributions have been thoroughly studied [7], [8], [9], on the basis of the IRA method. A more general mixture model has been proposed in [34] based on the Pearson type VII distribution (includes the  $t$ -distribution as a special case). Moreover, as the transformed coefficients in the wavelet domain tend to be Laplace distributed, a mixture of the Laplace distributions has been proposed in [10] for image denoising. Its more general version, a mixture of hyperbolic distributions, has also been recently introduced in [11]. The above distributions belong to the *scale mixture of normals* class, which can be regarded as a convolution of a Gamma distribution and a Gaussian distribution, and ensures the convergence of the IRA. On the other hand, Wiesel proved the convergence of the IRA in [35] via the concept of geodesic convexity of Riemannian manifold, and Zhang *et al.* further relaxed the convergence conditions in [14]. The work [15] proves similar results from another perspective

of the Riemannian manifold, which also states that the IRA cannot ensure a universal convergence for all EMMs. In other words, for other elliptical distributions, the convergence is no longer guaranteed. Despite several attempts, current EMMs, including [36], [37], [38], are rather of an *ad hoc* nature.

Besides the IRA method for solving several EMMs, gradient-based numerical algorithms typically rest upon additional techniques that only work in particular situations (e.g., gradient reduction [39], re-parametrisation [40] and Cholesky decomposition [41], [42]). Recently, Hosseini and Sra directly adopted a Riemannian manifold method for estimating the GMM, which provided an alternative to the traditional EM algorithm in the GMM problem [16], [17]. However, their method fails to retain the optimum in the EMM problem. We thus propose a universal scheme to consistently and stably achieve the optimum at a fast speed, which acts as a “necessity” instead of an “alternative” in the EMM problem, as the IRA algorithm may not converge.

## III. MANIFOLD OPTIMISATION FOR THE EMM

In this section, we shall first justify the Riemannian metrics of elliptical distributions in Section III-A, followed by a lay out of the EMM problem, and the introduction of the proposed method in Section III-B. Finally, a type of regularisation on the EMMs is shown in Section III-C, which includes the *mean-shift* algorithm as a special case.

### A. Statistical metrics for elliptical distributions

Although there are various metrics designed for measuring the distance between matrices [43], [44], [45], [46], not all of them arise from the smooth varying inner product (i.e., Riemannian metrics), which would consequently give a “true” geodesic distance. One of the widely employed Riemannian metrics is the intrinsic metric  $\text{tr}(d\Sigma\Sigma^{-1}d\Sigma\Sigma^{-1})$ , which can be obtained via the “entropy differential metric” [47] of two multivariate Gaussian distributions. The entropy related metric was later used by Hiai and Petz to define the Riemannian metric for positive definite matrices [48]. In this paper, we follow the work of [48] to calculate the corresponding Riemannian metrics for the elliptical distributions.

**Lemma 1.** Consider the class of elliptical distributions  $\mathcal{E}(\mathbf{x}|\boldsymbol{\mu}, \Sigma, g)$ . Then, the Riemannian metric for the mean is given by

$$ds^2 = \left[ \frac{4}{M} \int_0^\infty t \left( \frac{g'(t)}{g(t)} \right)^2 p_{\mathcal{R}^2}(t) dt \right] d\boldsymbol{\mu}^T \Sigma^{-1} d\boldsymbol{\mu}, \quad (3)$$

and the Riemannian metric for the covariance by

$$ds^2 = \frac{1}{2} \text{tr}(d\Sigma\Sigma^{-1}d\Sigma\Sigma^{-1}). \quad (4)$$

*Proof.* Please see the Appendix-A.  $\square$

When estimating parameters of elliptical distributions, the mean vector and the covariance matrix need to be estimated simultaneously. An elegant strategy would be to incorporate the mean and the covariance into an augmented matrix with extra one dimension [12]. Such a strategy has also been

successfully employed in the work of [16], [17], which is called ‘‘reformulation trick’’. Thus, based on the metrics of Lemma 1, we have the following relationship related to the reformulation.

**Lemma 2.** *Consider the class of elliptical distributions,  $\mathcal{E}(\mathbf{y}|\mathbf{0}, \tilde{\Sigma}, g)$ . Then, upon reformulating  $\mathbf{y}$  and  $\tilde{\Sigma}$  as*

$$\mathbf{y} = [\mathbf{x}^T, 1]^T, \quad \tilde{\Sigma} = \begin{pmatrix} \Sigma + \lambda \boldsymbol{\mu} \boldsymbol{\mu}^T & \lambda \boldsymbol{\mu} \\ \lambda \boldsymbol{\mu}^T & \lambda \end{pmatrix} \quad (5)$$

the following Riemannian metric and equation follow

$$\begin{aligned} ds^2 &= \text{tr}(d\tilde{\Sigma}\tilde{\Sigma}^{-1}d\tilde{\Sigma}\tilde{\Sigma}^{-1}) \\ &= \lambda d\boldsymbol{\mu}^T \Sigma^{-1} d\boldsymbol{\mu} + \frac{1}{2} \text{tr}(d\Sigma \Sigma^{-1} d\Sigma \Sigma^{-1}) + \frac{1}{2} (\lambda^{-1} d\lambda)^2. \end{aligned} \quad (6)$$

*Proof.* The proof is a direct extension to that in [49], in which only the Gaussian case is proved. We omit the proof here.  $\square$

From this lemma, we can inspect the relationship between manifolds with and without such a reformulation, which provides another perspective in understanding the reformulation.

**Remark.** *In Lemma 2, there is a mismatch between the two manifolds, due to the term  $\frac{1}{2}(\lambda^{-1}d\lambda)^2$ . When restricted to the Gaussian case, we will shortly see that the gradient on  $\lambda$  vanishes when optimising  $\tilde{\Sigma}$ , i.e.,  $d\lambda = 0$ . In this case, manifold optimisation on  $\tilde{\Sigma}$  is performed under the same metric as a simultaneous optimisation on a product manifold of the mean and the covariance, which leads to the success of [16], [17] in solving GMMs. However, this property does not hold for general EMMs.*

## B. Manifold optimisation on the EMM

Generally, we assume that the EMM consists of  $K$  mixtures, each elliptically distributed. To make the proposed EMM flexible enough to capture inherent structures in data, in our framework it is not necessary for every elliptical distribution to have the same density generator (denoted by  $\mathcal{E}_k(\mathbf{x}|\boldsymbol{\mu}_k, \Sigma_k, g_k)$ ). In finite mixture models, the probability of choosing the  $k$ -th mixture is denoted by  $\pi_k$ , so that  $\sum_{k=1}^K \pi_k = 1$ . For a set of i.i.d samples  $\mathbf{x}_n$ ,  $n = 1, 2, 3, \dots, N$ , the negative log-likelihood can be obtained as

$$J = -\sum_{n=1}^N \ln \sum_{k=1}^K \pi_k c_M \det(\Sigma_k)^{-\frac{1}{2}} g_k((\mathbf{x}_n - \boldsymbol{\mu}_k)^T \Sigma_k^{-1} (\mathbf{x}_n - \boldsymbol{\mu}_k)). \quad (7)$$

The estimation of  $\pi_k$ ,  $\boldsymbol{\mu}_k$  and  $\Sigma_k$  requires the minimisation of  $J$  in (7). By setting the derivatives of  $J$  to 0, we have the following equations,

$$\begin{aligned} \pi_k &= \frac{\sum_{n=1}^N \xi_{nk}}{N}, \quad \boldsymbol{\mu}_k = \frac{\sum_{n=1}^N \xi_{nk} \psi_k(t_{nk}) \mathbf{x}_n}{\sum_{n=1}^N \xi_{nk} \psi_k(t_{nk})}, \\ \Sigma_k &= -2 \frac{\sum_{n=1}^N \xi_{nk} \psi_k(t_{nk}) (\mathbf{x}_n - \boldsymbol{\mu}_k) (\mathbf{x}_n - \boldsymbol{\mu}_k)^T}{\sum_{n=1}^N \xi_{nk}}, \end{aligned} \quad (8)$$

where  $\xi_{nk} = \frac{\mathcal{E}_k(\mathbf{x}_n|\boldsymbol{\mu}_k, \Sigma_k, g_k) \pi_k}{\sum_{k=1}^K \mathcal{E}_k(\mathbf{x}_n|\boldsymbol{\mu}_k, \Sigma_k, g_k) \pi_k}$  is the posterior distribution of latent variables;  $t_{nk} = (\mathbf{x}_n - \boldsymbol{\mu}_k)^T \Sigma_k^{-1} (\mathbf{x}_n - \boldsymbol{\mu}_k)$  is the Mahalanobis distance;  $\psi_k(t_{nk}) = g_k'(t_{nk})/g_k(t_{nk})$  almost

acts as an M-estimator for most heavily-tailed elliptical distributions, which decreases to 0 when the Mahalanobis distance  $t_{nk}$  increases to infinity. It is obvious that the solutions  $\pi_k$ ,  $\boldsymbol{\mu}_k$  and  $\Sigma_k$  are intertwined by  $\xi_{nk}$  and  $t_{nk}$ , which prevents a closed-form solution<sup>1</sup> of (7). By iterating (8), this results to an EM-type solver, which is exactly the IRA algorithm. However, the convergence of the IRA is not guaranteed for general EMMs [12].

On the other hand, when directly estimating the reformulated EMM, i.e.,  $\mathcal{E}_k(\mathbf{y}|\mathbf{0}, \tilde{\Sigma}_k, g_k)$ , similarly, we arrive at

$$\tilde{\pi}_k = \frac{\sum_{n=1}^N \tilde{\xi}_{nk}}{N}, \quad \tilde{\Sigma}_k = -2 \frac{\sum_{n=1}^N \tilde{\xi}_{nk} \psi_k(\tilde{t}_{nk}) \mathbf{y}_n \mathbf{y}_n^T}{\sum_{n=1}^N \tilde{\xi}_{nk}}, \quad (9)$$

where  $\tilde{t}_{nk} = \mathbf{y}_n^T \tilde{\Sigma}_k^{-1} \mathbf{y}_n$  and  $\tilde{\xi}_{nk} = \frac{\mathcal{E}_k(\mathbf{y}_n|\mathbf{0}, \tilde{\Sigma}_k, g_k) \tilde{\pi}_k}{\sum_{k=1}^K \mathcal{E}_k(\mathbf{y}_n|\mathbf{0}, \tilde{\Sigma}_k, g_k) \tilde{\pi}_k}$ . We can also decompose  $\tilde{\Sigma}_k$  to obtain the corresponding solutions  $\boldsymbol{\mu}_k$  and  $\Sigma_k$  as well as  $\lambda_k = -2 \frac{\sum_{n=1}^N \tilde{\xi}_{nk} \psi_k(\tilde{t}_{nk})}{\sum_{n=1}^N \tilde{\xi}_{nk}}$  from (5). However, we can easily find that the solutions are generally different from those of (8), which means that the optimisation on the direct reformulation may result in wrong solutions in the EMM problems. The only exception is when solving the GMM, where  $\psi_k(t_{nk}) = -1/2$ ,  $\lambda_k \equiv 1$ , and the manifold with the reformulation is same as the original one.

To retain the same optimum as the original problem, we introduce a new parameter  $c_k$ , which aims to mitigate the mismatch of the reformulated manifold brought by  $\lambda_k$ . The same optimum is ensured in the following theorem:

**Theorem 1.** *The optimisation of  $\pi_k$ ,  $\tilde{\Sigma}_k$  and  $c_k$  on the following re-designed cost*

$$\tilde{J} = -\sum_{n=1}^N \ln \sum_{k=1}^K \pi_k \cdot c_M \cdot (c_k \det(\tilde{\Sigma}_k))^{-1/2} g_k(\mathbf{y}_n^T \tilde{\Sigma}_k^{-1} \mathbf{y}_n - c_k) \quad (10)$$

has the same optimum as those in (8):

$$\begin{aligned} \pi_k &= \frac{\sum_{n=1}^N \xi_{nk}}{N}, \quad c_k = \frac{1}{\lambda_k} = -\frac{\sum_{n=1}^N \xi_{nk}}{2 \sum_{n=1}^N \xi_{nk} \psi_k(t_{nk})} \\ \tilde{\Sigma}_k &= -2 \frac{\sum_{n=1}^N \xi_{nk} \psi_k(t_{nk}) \mathbf{y}_n \mathbf{y}_n^T}{\sum_{n=1}^N \xi_{nk}} \end{aligned} \quad (11)$$

*Proof.* Please see the Appendix-B.  $\square$

We optimise (10) in a product manifold of  $\tilde{\Sigma}_k$ ,  $\pi_k$  and  $c_k$ . For optimising  $\tilde{\Sigma}_k$ , on the basis of the metric in Section III-A, we calculate Riemannian gradient as  $\nabla_R \tilde{J} = \tilde{\Sigma}_k (\nabla_E \tilde{J}) \tilde{\Sigma}_k$ , where  $\nabla_E \tilde{J}$  is the Euclidean gradient of cost  $\tilde{J}$  via  $\partial \tilde{J} / \partial \tilde{\Sigma}_k$ . The retraction is then via  $\tilde{\Sigma}_k + \nabla_R \tilde{J} + 1/2 (\nabla_R \tilde{J}) \tilde{\Sigma}_k^{-1} (\nabla_R \tilde{J})$ , which is an approximation of the exponential mapping but exhibits enhanced computational feasibility. Finally, we employ the conjugate gradient descent [51] as a manifold solver.

<sup>1</sup>It should be pointed out that there are multiple solutions of (8) and the goal here is to find a local stationary point. Finding the global optima is difficult in mixture problems [50] and beyond the scope of this paper.

### C. Regularisation

We impose the inverse-Wishart prior distribution (i.e.,  $p_{\Sigma_k}(\Sigma_k) \propto \frac{1}{\det(\Sigma_k)^{v/2}} \exp(-\frac{v \text{tr}(\Sigma_k^{-1} \mathbf{S})}{2})$ ) to regularise the EMM, where  $v$  controls the freedom and  $\mathbf{S}$  is the prior matrix. The advantages of using a form of  $\text{tr}(\Sigma_k^{-1} \mathbf{S})$  are two-fold: it is strictly geodesic convex in  $\Sigma_k$  and the solutions are ensured to exist for any data configuration [52]. By utilising maximum a posterior on covariance matrices, we obtain the same solutions of  $\pi_k$  and  $\mu_k$  as those of (8), whereas  $\Sigma_k$  is changed to

$$\Sigma_k = \frac{-2 \cdot \sum_{n=1}^N \xi_{nk} \psi_k(t_{nk}) (\mathbf{x}_n - \mu_k) (\mathbf{x}_n - \mu_k)^T + v \mathbf{S}}{\sum_{n=1}^N \xi_{nk} + v}. \quad (12)$$

Similar to Theorem 1, the following proposition can be obtained for the reformulation with regularisations.

**Proposition 1.** *The optimisation of  $\pi_k$ ,  $\tilde{\Sigma}_k$  and  $c_k$  on the following function*

$$\tilde{J}_r = \tilde{J} + \sum_{k=1}^K (c_k \det(\tilde{\Sigma}_k))^{-v/2} \exp\left(-\frac{v \text{tr}(\tilde{\Sigma}_k^{-1} \tilde{\mathbf{S}})}{2}\right), \quad (13)$$

achieves the same optimal  $\Sigma_k$  as in (12) and the same  $\pi_k$  and  $\mu_k$  as in (8), where  $\tilde{\mathbf{S}} = \begin{bmatrix} \mathbf{S} & \mathbf{0} \\ \mathbf{0} & 0 \end{bmatrix}$ . The optimal  $c_k$  and  $\lambda_k$  are

$$c_k = \frac{1}{\lambda_k} = -\frac{\sum_{n=1}^N \xi_{nk} + v}{2 \sum_{n=1}^N \xi_{nk} \psi_k(t_{nk})}. \quad (14)$$

*Proof.* The proof is analogous to that of Theorem 1 and we omit its proof here.  $\square$

**Remark.** In (12), it can be seen that when  $v \rightarrow \infty$ ,  $\Sigma_k \rightarrow \mathbf{S}$ . Furthermore, when  $\mathbf{S} = \mathbf{I}_M$ ,  $\Sigma_k = \sigma^2 \mathbf{I}_M$ , the estimation of  $\mu_k$  in (8) becomes  $\frac{\sum_{n=1}^N \xi_{nk} \psi_k(\sigma^{-2} \|\mathbf{x}_n - \mu_k\|^2) \mathbf{x}_n}{\sum_{n=1}^N \xi_{nk} \psi_k(\sigma^{-2} \|\mathbf{x}_n - \mu_k\|^2)}$ , which is the basic mean-shift algorithm with soft thresholds. Furthermore, when  $\mathbf{S} = \mathbf{I}_M$ ,  $\Sigma_k = \mathbf{I}_M$  and  $\psi_k(t_{nk}) = -1/2$  (the GMM), it then turns to the basic  $k$ -means algorithm. This all demonstrates that the EMM is a flexible framework in our regularisation settings and one can choose  $v$  and  $\mathbf{S}$  to achieve different models.

## IV. INFLUENCE FUNCTIONS OF THE EMM

Robustness properties of a single elliptical distribution (or more generally, an M-estimator) have been extensively studied [53], [54], [2], [55], typically from the perspective of influence functions (IFs) [56]. The IF is an important metric in quantifying the impact of an infinitesimal fraction of outliers on the estimations, which captures the local robustness. However, to the best of our knowledge, there exists no work on the IF of mixture models, especially for the EMMs. To calculate the IFs, we utilise  $\mathbf{x}_0$  to denote point-mass outliers, which means that these outliers are point-mass distributed at  $\mathbf{x}_0$  [2]. We also explicitly write the posterior distribution of latent variables as a function of  $\mathbf{x}$  ( $\xi_j(\mathbf{x}) = \frac{\mathcal{E}_j(\mathbf{x} | \mu_j, \Sigma_j, g_j) \pi_j}{\sum_{k=1}^K \mathcal{E}_k(\mathbf{x} | \mu_k, \Sigma_k, g_k) \pi_k}$ ), because in robustness analysis, we need to quantify it with respect of outliers. For simplicity,  $t_j$  is also defined as the Mahalanobis distance

$(\mathbf{x} - \mu_j)^T \Sigma_j^{-1} (\mathbf{x} - \mu_j)$  and  $\mathbb{E}[\cdot]$  is the expectation over the true distribution of  $\mathbf{x}$ . Then, our analysis on the IFs is based on the following two lemmas.

**Lemma 3.** *Consider the mixture of elliptical distributions,  $\mathcal{E}_k(\mathbf{x} | \mu_k, \Sigma_k, g_k)$ . When data are well separated, upon denoting  $(\mathbf{x}_0 - \mu_j)$  by  $\bar{\mathbf{x}}_0$  for the  $j$ -th cluster, its IF is given in (15) at the bottom,*

$$\begin{aligned} \mathcal{I}_{\Sigma_j}(\mathbf{x}_0) = & -\frac{\xi_j(\mathbf{x}_0) \psi_j(\bar{\mathbf{x}}_0^T \Sigma_j^{-1} \bar{\mathbf{x}}_0)}{w_2} \bar{\mathbf{x}}_0 \bar{\mathbf{x}}_0^T \\ & + \Sigma_j^{\frac{1}{2}} \left[ \frac{2w_1 \cdot \xi_j(\mathbf{x}_0) \psi_j(\bar{\mathbf{x}}_0^T \Sigma_j^{-1} \bar{\mathbf{x}}_0) \bar{\mathbf{x}}_0^T \Sigma_j^{-1} \bar{\mathbf{x}}_0 + w_2 \cdot \xi_j(\mathbf{x}_0) \mathbf{I}}{2(Mw_1 - w_2)w_2} \right] \Sigma_j^{\frac{1}{2}}, \end{aligned} \quad (15)$$

where  $w_1$  and  $w_2$  are constants (irrelevant to the outlier  $\mathbf{x}_0$ ) given by

$$\begin{aligned} w_1 = & \frac{\mathbb{E}[(\xi_j(\mathbf{x}) - \xi_j^2(\mathbf{x})) \psi_j^2(t) t^2] + \mathbb{E}[\xi_j(\mathbf{x}) \psi_j'(t) t^2]}{M(M+1)} \\ & + \frac{\mathbb{E}[(\xi_j(\mathbf{x}) - \xi_j^2(\mathbf{x})) \psi_j(t) t]}{M} + \frac{\mathbb{E}[\xi_j(\mathbf{x}) - \xi_j^2(\mathbf{x})]}{4}, \quad (16) \\ w_2 = & \frac{\pi_j}{2} - \frac{\mathbb{E}[(\xi_j(\mathbf{x}) - \xi_j^2(\mathbf{x})) \psi_j^2(t) t^2] + \mathbb{E}[\xi_j(\mathbf{x}) \psi_j'(t) t^2]}{M(M+1)}. \end{aligned}$$

**Lemma 4.** *Consider the mixture of elliptical distributions,  $\mathcal{E}_k(\mathbf{x} | \mu_k, \Sigma_k, g_k)$ . When data are well separated, for the  $j$ -th cluster, its IF on the mean is given by*

$$\mathcal{I}_{\mu_j}(\mathbf{x}_0) = \frac{1}{w_3} \xi_j(\mathbf{x}_0) \psi_j(\mathbf{x}_0) (\mathbf{x}_0 - \mu_j), \quad (17)$$

where  $w_3$  is a constant (irrelevant to the outlier  $\mathbf{x}_0$ ) given by

$$\begin{aligned} w_3 = & \frac{2\mathbb{E}[\xi_j(\mathbf{x}) \psi_j'(t) t]}{M} \\ & + \mathbb{E}[\xi_j(\mathbf{x}) \psi_j(t)] + \frac{2\mathbb{E}[(\xi_j(\mathbf{x}) - \xi_j^2(\mathbf{x})) \psi_j^2(t) t]}{M}. \end{aligned} \quad (18)$$

Proofs of the two lemmas are provided in the Appendices-C and D. The actual and theoretical IF curves of four EMMs are plotted in Fig. 1, showing that in practice the robustness of the EMMs can be well captured by our theoretical bounds.

More importantly, the robustness of the EMM can also be analysed from Lemmas 3 and 4. Specifically, when  $\mathbf{x}_0 \rightarrow \infty$ ,  $\mathcal{I}_{\Sigma_j}(\mathbf{x}_0)$  is bounded (defined as *covariance robust*) only when  $\psi_j(t)t$  is bounded for  $t \rightarrow \infty$ , which leads to bounded  $\psi_j(\bar{\mathbf{x}}_0^T \Sigma_j^{-1} \bar{\mathbf{x}}_0) \bar{\mathbf{x}}_0^T \Sigma_j^{-1} \bar{\mathbf{x}}_0$  in (15). Likewise, bounded  $\mathcal{I}_{\mu_j}(\mathbf{x}_0)$  (defined as *mean robust*) requires bounded  $\psi_j(t)\sqrt{t}$ , which is slightly more loose than the requirement of *covariance robust*. For example, in Fig. 1, by inspecting the boundedness of the curves, we can find that the Gaussian and the GG1.5 mixtures are neither *covariance robust* and *mean robust*, while the Cauchy mixtures are both *covariance robust* and *mean robust*. For the Laplace mixtures, they are not *covariance robust* but are *mean robust*, which shows that the *covariance robust* is more stringent than the *mean robust*. Thus, the developed bounds provide an extremely feasible and convenient treatment in qualifying or designing the robustness within EMMs.

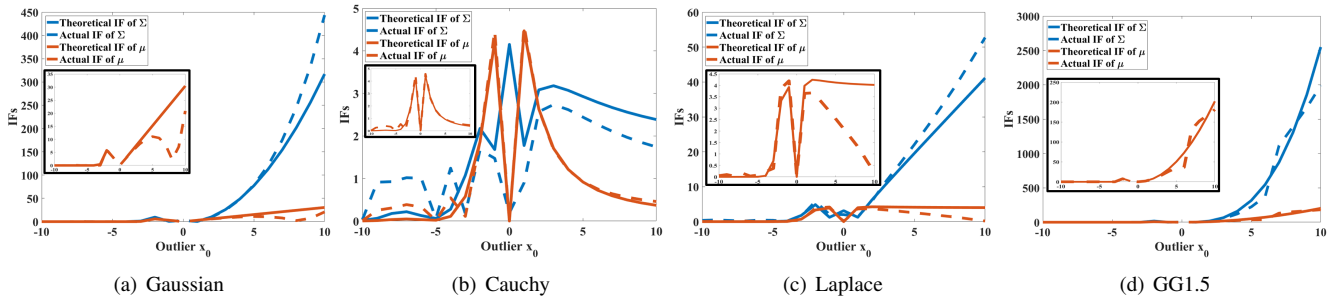


Fig. 1. For reproducibility, we follow the work of [57] to generate 3 one-dimensional clusters using the inverse of the Gaussian cumulative distribution function. The 3 clusters are centred at  $\mu_1 = 0$ ,  $\mu_2 = -5$  and  $\mu_3 = -10$ , and IF curves for  $\mu_1$  are illustrated. The mixture distributions are the Gaussian, the Cauchy, the Laplace and the GG1.5 in Table I. The theoretical bounds are plotted in solid lines and the actual IFs are plotted in dotted lines. The zoomed versions of the IFs of the mean are given in the black box of each figure.

## V. EXPERIMENTAL RESULTS

Our experimental settings are first detailed in Section V-A. We then employ in Section V-B two toy examples to illustrate the flexibility of EMMs in capturing different types of data. This also highlights the virtues of our method in universally solving EMMs. In Section V-C, we systematically compare our EMM solver with other baselines on the synthetic dataset, followed by a further evaluation on the image data of BSDS500 in Section V-D.

### A. Parameter settings and environments

**Baselines:** We compared the proposed method (**Our**) with the regular manifold optimisation (**RMO**) method without reformulation (i.e., updating  $\mu_k$  and  $\Sigma_k$  separately) and the **IRA** method, by optimising different EMMs over various data structures. It should be pointed out that the IRA includes a range of existing works on solving certain EMMs, e.g., the standard EM algorithm for the Gaussian distribution, [7] for the  $t$ -distribution and [11] for the hyperbolic distribution. Besides, the convergence criterion in all the experiments was set by the cost decrease of adjacent iterations of less than  $10^{-10}$ . For our method and the RMO, that involve manifold optimisation, we have utilised the default conjugate gradient solver in the Manopt toolbox [58].

**Performance objectives:** We compared our method with the RMO and IRA methods by comprehensively employing 8 different elliptical distributions as components within EMMs. We listed the 8 elliptical distributions in Table I, with their properties provided in Table II. We should also point out that the non-geodesic elliptical distributions cannot be solved by the IRA method [14], [15]. In contrast, as shown below, our method can provide a stable and fast solution even for the non-geodesic elliptical distributions.

**Synthetic datasets:** In total, we generated  $3 \times 2 = 6$  types of synthetic datasets, whereby  $M$  and  $K$  were set in pairs to  $\{8, 8\}$ ,  $\{16, 16\}$ , and  $\{64, 64\}$ ;  $c$  and  $e$  were set in pairs to  $\{10, 10\}$  and  $\{0.1, 1\}$  to represent the two extreme cases. Each synthetic dataset contained different mixtures of Gaussian distributions, with 10,000 samples in total ( $N = 10,000$ ). Their means and covariances were randomly chosen, except for their *separation*  $c$  and *eccentricity*

$e$  [33], [59], which were controlled to comprehensively evaluate the proposed method under various types of data structures. The separation,  $c$ , of two clusters  $k_1$  and  $k_2$  is defined as  $\|\mu_{k_1} - \mu_{k_2}\|^2 \geq c \cdot \max\{\text{tr}(\Sigma_{k_1}), \text{tr}(\Sigma_{k_2})\}$ , and the eccentricity,  $e$ , is defined as a ratio of the largest and the smallest eigenvalue of the covariance matrix within one cluster. The smaller value of  $c$  indicates the larger overlaps between clusters; the smaller value of  $e$  means more spherically distributed clusters. For each test case (i.e., for each method and for each EMM), we repeatedly ran the optimisation for 50 times, with random initialisations. Finally, we recorded average values of the iterations, the computational time and the final cost. When the optimisation failed, i.e., converging to singular covariance matrices or infinite negative likelihood, we also recorded and calculated the optimisation fail ratio within the 50 initialisations for each test case to evaluate the stability in optimisation.

**BSDS500 dataset:** Finally, we compared the three methods for image data. Specifically, all the 500 pictures in the Berkeley segmentation dataset BSDS500 [60] were tested and reported in our test. Each optimisation was initialised by the  $k$ -means++ in the vl-feat toolbox [61]. The cost difference, cost, iterations and computational time were recorded for all the 500 pictures.

### B. Toy examples

Before comprehensively evaluating our method, we first provide two illustrations on the basis of flower-shaped data with 4 clusters ( $N = 10,000$ ) (shown in Fig. 2-(a)), to illustrate the flexibility of the EMMs via our method: (i) Adding 100% uniform noise (i.e., 10,000 noisy samples), as shown in Fig. 2-(b); (ii) Replacing two clusters by the Cauchy samples with the same mean and covariance matrices, as shown in Fig. 2-(c). The five distributions that were chosen as components in EMMs are shown in Fig. 2-(d).

The optimised EMMs are shown in Fig. 3. From this figure, we find that the GMM is inferior in modelling noisy or unbalanced data. This is mainly due to its lack of robustness, and thus similar results can be found in another non-robust EMM, i.e., the GG1.5. In contrast, for a robust EMM, such as the Cauchy and the Laplace, the desirable estimations



TABLE I  
DETAILS OF 8 ELLIPTICAL DISTRIBUTIONS FOR ASSESSMENTS

	Gaussian	Cauchy	GG1.5	Logistic
$g(t)$ of (2)	$g(t) \propto \exp(-0.5t)$	$g(t) \propto (1+t)^{-(M+1)/2}$	$g(t) \propto \exp(-0.5t^{1.5})$	$g(t) \propto \frac{\exp(-t)}{(1+\exp(-t))^2}$
	Laplace	Weib0.9	Weib1.1	Gamma1.1
$g(t)$ of (2)	$g(t) \propto \frac{\mathcal{K}_{(1-0.5M)(\sqrt{2t})}}{\sqrt{0.5t}^{0.5M-1}}$	$g(t) \propto t^{-0.1} \exp(-0.5t^{0.9})$	$g(t) \propto t^{0.1} \exp(-0.5t^{1.1})$	$g(t) \propto t^{0.1} \exp(-0.5t)$
Note:	$\mathcal{K}_x(y)$ is the modified Bessel function of the second kind.			

TABLE II  
PROPERTIES OF THE 8 ELLIPTICAL DISTRIBUTIONS EMPLOYED FOR EVALUATIONS

	Gaussian	Cauchy	Laplace	GG1.5	Logistic	Weib0.9	Weib1.1	Gamma1.1
Covariance Robust	No	Yes	No	No	No	No	No	No
Mean Robust	No	Yes	Yes	No	No	No	No	No
Heavily Tailed	No	Yes	Yes	No	No	Yes	No	No
Geodesic Convex	Yes	Yes	Yes	Yes	Yes	Yes	No	No

are ensured in both cases. Therefore, a universal solver is crucial as it enables flexible EMMs can be well optimised for different types of data.

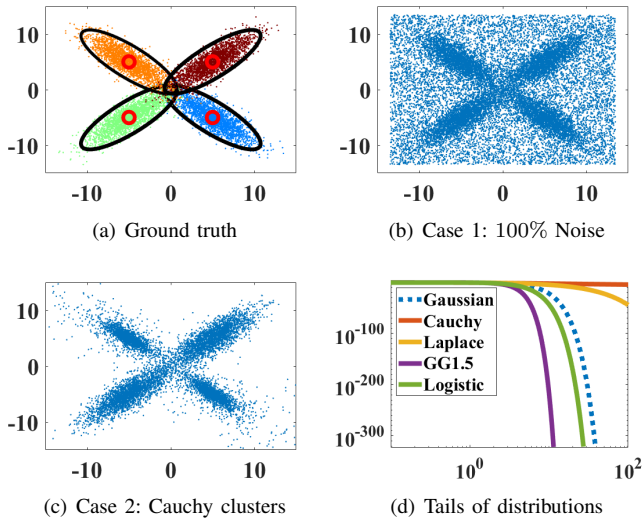


Fig. 2. Toy examples consisting of 4 Gaussian sets. (a) Data structure; the red circles represent the mean values at  $(5, 5)$ ,  $(5, -5)$ ,  $(-5, 5)$  and  $(-5, -5)$ , and the black circles denote covariance ellipses including 95% data samples of each Gaussian distribution. (b) Test case with data being added 100% uniform noisy samples. (c) Test case of data that consist of two Gaussian and two Cauchy sets. (d) Tails of the distributions which were utilised in this test. It needs to be pointed out that the Cauchy samples in (c) are spread in a wide range, so that we show (c) within  $(\pm 15, \pm 15)$  for illustration convenience.

We further plot the iteration numbers against the average cost difference of our, IRA and RMO methods when optimising the two cases in Fig. 4 and 5. Note that for the need of illustrations [16], the cost difference is defined by the absolute difference between the cost of each iteration and the relatively “optimal” cost, which was obtained by choosing the lowest value among the final costs of the three methods. From the two figures, it is obvious that the proposed method converges with the least number of iterations. Moreover, although one

iteration of our method takes longer time than that of the IRA method due to the line search within our method, the overall computational time of our method is comparable to that of the IRA method. As shown in the next section, our method even performs much faster in terms of computational time than the IRA for higher dimensions and larger numbers of clusters ( $M > 2$  and  $K > 4$ ).

### C. Evaluations over the synthetic datasets

We here systematically evaluate our method under the synthetic dataset described in Section V-A. For each dataset, we have  $8 \times 3 = 24$  test cases, i.e., 8 types of EMMs for the 3 methods. The 8 types of EMMs include 7 types of elliptical distributions and the other one (denoted as Mix) is composed by half the number of Cauchy distributions and the other half of Gaussian distributions. Table III shows the overall result averaged across dimensions  $M$  and  $K$  for the 8 EMMs. As can be seen from Table III, our method enjoys the fastest convergence speed in terms of both iterations and computation time, and it also obtains the minimum cost. It can also be found that datasets with more overlaps (i.e.,  $\{c = 0.1, e = 1\}$ ) take a longer time to optimise, whereby iterations and computational time increase for all the 3 methods. On the other hand, by comparing the results of our method and those of the RMO method, we can obviously see a significant improvement on both convergence speed and final minimum, which verifies the effectiveness of our reformulation technique.

We further provide the details of comparisons of different  $M$  and  $K$  in Table IV, where 3 EMMs and  $\{c = 10, e = 10\}$  were reported due to the space limitation and similar results can be found for other EMMs and settings of Table III. We can see from this table that the superior performance of our method is consistent for different dimensions  $M$  and cluster numbers  $K$ . We can easily find from this table that our method achieves the minimum numbers of iterations as well as computational time. More importantly, the standard deviations for the iterations and computational time of our method are almost the lowest, which means that our method is able to

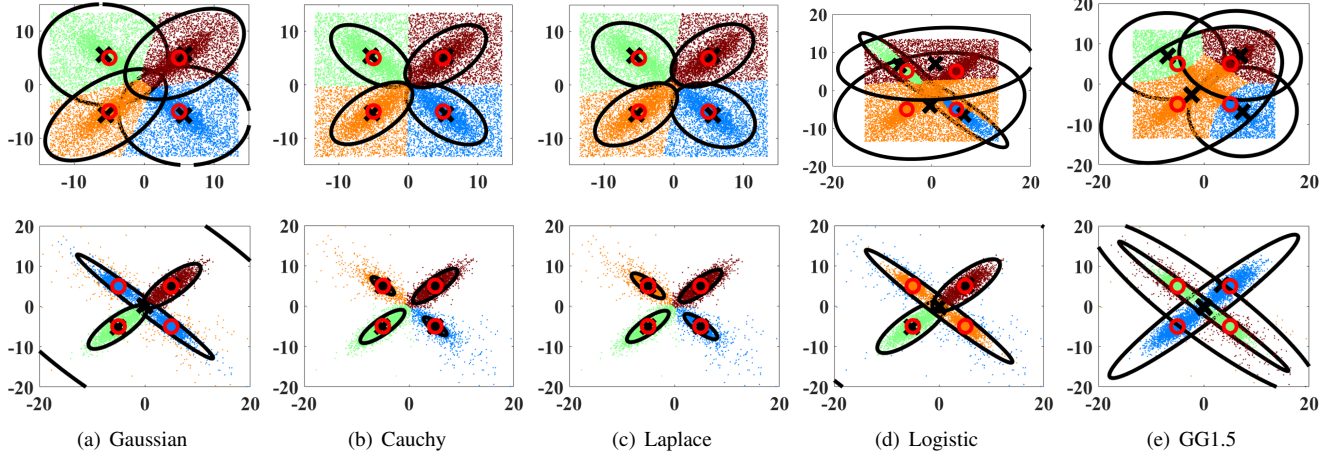


Fig. 3. Optimisation results of the proposed method across the 5 EMMs. The top row shows the results in Case 1 and the bottom row show the results of Case 2. The red circles denote the ground-truth as shown in Fig. 2-(a), whilst the black crosses and ellipses represent the estimated mean values and covariance matrices. The colour of each sample is corresponding to that of Fig. 2-(a), and is classified by selecting the maximum posterior among the 4 clusters.

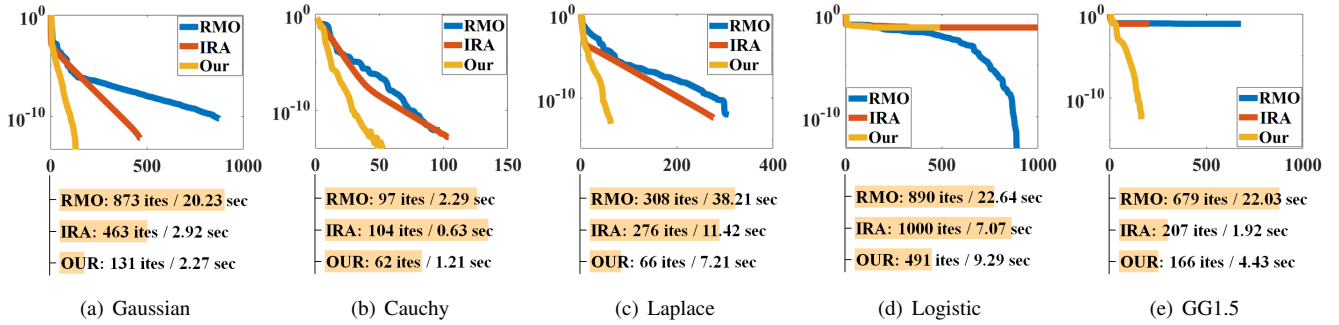


Fig. 4. Cost difference against numbers of iterations of the 5 EMMs within Case 1. The top figures show the cost difference against the iterations optimised via Our, IRA and RMO methods. The bottom quantities are the final convergence speed in terms of the number of iterations and execution time (ites/sec).

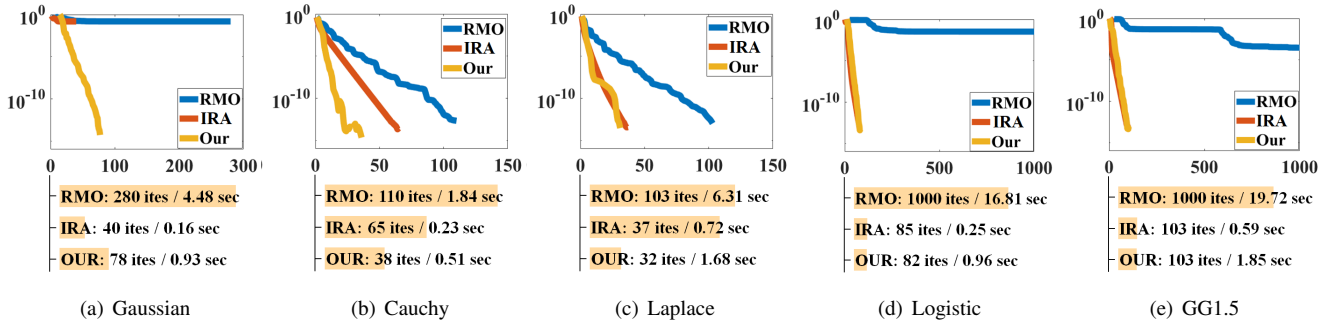


Fig. 5. Cost difference against numbers of iterations of the 5 EMMs within Case 2. The top figures show the cost difference against the iterations optimised via Our, IRA and RMO methods. The bottom quantities are the final convergence speed in terms of the number of iterations and execution time (ites/sec).

stably optimise the EMMs. With the increase of  $M$  and  $K$ , our method consistently achieves the best performance of the average costs with 0% fail ratio. In contrast, the IRA became extremely unstable. For examples, for  $\{M = 64, K = 64\}$ , the IRA failed 90% when optimising the Gaussian mixture. It even totally failed (100%) for the Cauchy mixture. For the Logistic mixture, it failed 70%. When compared to our and RMO methods, we see an increase of stability when using

manifold optimisation. The RMO, however, took extremely large computational complexity ( $> 900$  iterations and  $> 4000$  seconds when  $M = 64, K = 64$ ). On the other hand, our method consistently and stably optimised the EMMs with the fastest convergence speed and lowest cost.



TABLE III  
OVERALL RESULTS AVERAGED ACROSS  $M$  AND  $K$  OF 8 TYPES OF EMMs OPTIMISED BY OUR, IRA AND RMO.

$c = 10, e = 10$		Gaussian	Cauchy	GG1.5	Logistic	Weib0.9	Weib1.1	Gamma1.1	Mix
Our	Ite. / T. (s)	<b>108 / 40.3</b>	<b>135 / 34.5</b>	<b>219 / 160</b>	<b>113 / 43.2</b>	<b>158 / 37.8</b>	<b>139 / 56.5</b>	<b>138 / 38.3</b>	<b>132 / 51.8</b>
	Cost	64.5	<b>65.6</b>	<b>69.8</b>	47.8	<b>64.4</b>	<b>64.4</b>	<b>64.4</b>	<b>67.5</b>
IRA	Ite. / T. (s)	367 / 90.0	—	—	428 / 249	310 / 46.8	—	—	—
	Cost	66.2	—	—	49.0	64.5	—	—	—
RMO	Ite. / T. (s)	658 / 1738	848 / 1590	796 / 1435	744 / 1651	825 / 1806	773 / 1625	760 / 1550	711 / 1547
	Cost	<b>64.3</b>	65.8	71.6	<b>47.5</b>	64.4	64.5	64.5	66.8
$c = 0.1, e = 1$		Gaussian	Cauchy	GG1.5	Logistic	Weib0.9	Weib1.1	Gamma1.1	Mix
Our	Ite. / T. (s)	<b>693 / 201</b>	<b>424 / 99.9</b>	<b>581 / 100</b>	<b>734 / 242</b>	<b>686 / 119</b>	<b>655 / 111</b>	<b>664 / 94.6</b>	<b>470 / 65.7</b>
	Cost	<b>40.0</b>	<b>41.0</b>	<b>39.8</b>	<b>23.5</b>	<b>39.1</b>	<b>40.1</b>	<b>40.1</b>	<b>39.2</b>
IRA	Ite. / T. (s)	—	—	—	—	711 / 101	—	—	—
	Cost	—	—	—	—	40.6	—	—	—
RMO	Ite. / T. (s)	1000 / 1707	956 / 1661	898 / 1206	963 / 1508	969 / 1632	975 / 1744	958 / 1561	917 / 1505
	Cost	40.4	41.5	42.1	23.8	40.3	40.5	40.4	40.4
Note:		T. (s): Time (seconds); Ite.: Iteration numbers; —: Singularity or infinity in either $M = 8, M = 16$ or $M = 64$ .							

TABLE IV  
DETAILED COMPARISONS AMONG OUR, IRA AND RMO ON OPTIMISING 3 EMMs IN THE CASE OF  $c = 10$  AND  $e = 10$

(M, K)		Gaussian			Cauchy			Logistic		
		Our	IRA	RMO	Our	IRA	RMO	Our	IRA	RMO
(8, 8)	T. (s)	<b>3.70 ± 5.44</b>	5.48 ± 4.13	4.23 ± 10.76	<b>2.23 ± 1.67</b>	3.04 ± 2.45	20.4 ± 10.6	<b>4.28 ± 4.60</b>	4.71 ± 4.08	18.9 ± 17.3
	Ite.	165 ± 240	538 ± 403	<b>122 ± 308</b>	<b>107 ± 81.3</b>	340 ± 275	640 ± 334	<b>177 ± 191</b>	463 ± 398	537 ± 489
	Co./Fa.	19.4 / 0%	19.6 / 0%	<b>19.3 / 0%</b>	<b>20.3 / 0%</b>	20.4 / 0%	20.3 / 0%	<b>14.9 / 0%</b>	15.0 / 0%	14.9 / 0%
(16, 16)	T. (s)	<b>15.8 ± 13.4</b>	28.8 ± 15.2	221 ± 78.3	<b>38.1 ± 34.5</b>	40.9 ± 18.2	260 ± 1.84	<b>15.7 ± 7.64</b>	23.6 ± 14.6	193 ± 115
	Ite.	<b>115 ± 94.0</b>	400 ± 207	853 ± 304	<b>272 ± 243</b>	570 ± 254	1000 ± 0.00	<b>115 ± 54.0</b>	325 ± 201	734 ± 433
	Co./Fa.	<b>37.7 / 0%</b>	38.0 / 0%	37.8 / 0%	<b>38.7 / 0%</b>	38.8 / 0%	39.0 / 0%	<b>28.6 / 0%</b>	28.8 / 0%	28.6 / 0%
(64, 64)	T. (s)	<b>101 ± 18.0</b>	236 ± 0.00	4988 ± 152	<b>63.2 ± 11.7</b>	—	4491 ± 1549	<b>110 ± 19.3</b>	720 ± 343	4741 ± 475
	Ite.	<b>45.8 ± 5.67</b>	163 ± 0.00	1000 ± 0.00	<b>26.9 ± 3.70</b>	—	902 ± 309	<b>49.3 ± 5.98</b>	497 ± 235	960 ± 121
	Co./Fa.	<b>136 / 0%</b>	141 / 90%	136 / 10%	<b>138 / 0%</b>	- / 100%	138 / 0%	<b>99.7 / 0%</b>	103 / 70%	<b>99.1 / 10%</b>
Note:		T. (s): Time (seconds); Ite.: Iteration numbers; Co.: Final cost; Fa.: Optimisation fail ratio; —: Singularity or infinity								

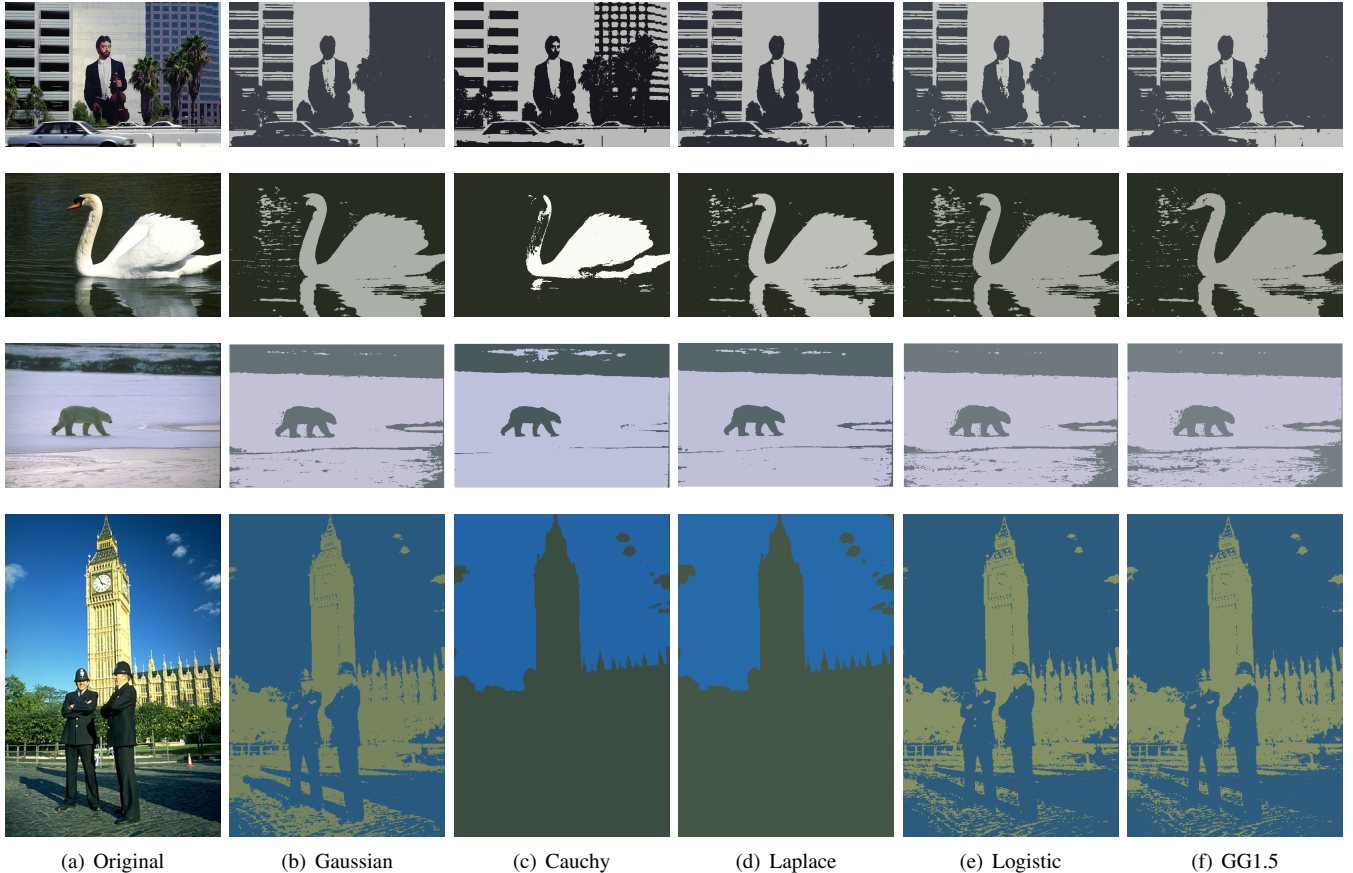


Fig. 6. Reconstructed images by our method when optimising the 5 EMMs.

TABLE V  
COMPARISONS AVERAGED OVER 500 PICTURES AMONG OUR, THE IRA AND THE RMO FOR ESTIMATING THE 5 EMMs

	Gaussian			Cauchy			Laplace			GG1.5			Logistic		
	Our	IRA	RMO	Our	IRA	RMO	Our	IRA	RMO	Our	IRA	RMO	Our	IRA	RMO
Iterations	<b>56</b>	234	954	<b>87</b>	390	939	<b>101</b>	288	962	<b>61</b>	224	982	<b>58</b>	239	965
Time (s)	<b>5.55</b>	11.8	165	<b>7.12</b>	16.8	159	<b>20.4</b>	42.2	486	<b>8.32</b>	14.4	205	<b>6.73</b>	13.3	177
Cost	<b>12.3</b>	12.3	12.3	<b>12.1</b>	12.4	12.3	<b>12.2</b>	12.2	12.3	<b>12.4</b>	12.4	12.4	<b>11.1</b>	11.1	11.2
SSIM [62]	0.5930			0.6052			0.6112			0.5813			0.5792		

#### D. BSDS500 dataset:

Convergence speed between Our, the IRA, and the RMO methods was compared over averaged results across the whole 500 pictures in BSDS500, as shown in Table V. Again, our method converged with the fastest speed and achieved the minimum cost error among the RMO and the IRA methods. We further show in Fig. 6 four reconstructed images via our method when optimising the five EMMs. Observe that the images reconstructed from the non-robust distributions (e.g., the Gaussian and the GG1.5 distributions) were more “noisy” than those from the robust distributions (e.g., the Cauchy and Laplace distributions); however, these may capture more details in images. Therefore, different EMMs can flexibly model data for different requirements or applications, and our method, compared to the existing methods, was able to consistently provide a fast, stable and superior optimisation.

## VI. CONCLUSIONS

We have proposed a general framework for a systematic analysis and universally optimisation of the EMMs, and have conclusively demonstrated that this equips EMMs with significantly enhanced flexibility and ease of use in practice. In addition to the general nature and the power of the proposed universal framework for EMMs, we have also verified both analytically and through simulations, that this provides a reliable and robust statistical tool for analysing the EMMs. Furthermore, we have proposed a general solver which consistently attains the optimum for general EMMs. Comprehensive simulations over both synthetic and real-world datasets validate the proposed framework, which is fast, stable and flexible.

## APPENDIX

### A. Proof of Lemma 1

We shall first calculate the Riemannian metric for the mean vectors. We note that Mitchell [63] first presented a similar result via an element-wise treatment, but here we provide a compact and consistent proof. Specifically, for the mean, the metric is obtained via the Fisher information as follows,

$$ds^2 = d\boldsymbol{\mu}^T \left[ \mathbb{E} \left[ \left( \frac{\partial \ln p_{\mathbf{x}}(\mathbf{x})}{\partial \boldsymbol{\mu}} \right) \cdot \left( \frac{\partial \ln p_{\mathbf{x}}(\mathbf{x})}{\partial \boldsymbol{\mu}} \right)^T \right] \right] d\boldsymbol{\mu}, \quad (19)$$

so that we obtain:

$$\begin{aligned} & \mathbb{E} \left[ \left( \frac{\partial \ln p_{\mathbf{x}}(\mathbf{x})}{\partial \boldsymbol{\mu}} \right) \cdot \left( \frac{\partial \ln p_{\mathbf{x}}(\mathbf{x})}{\partial \boldsymbol{\mu}} \right)^T \right] \\ &= 4 \int_{\mathbf{x}} \left( \frac{g'(t)}{g(t)} \right)^2 \boldsymbol{\Sigma}^{-1} (\mathbf{x} - \boldsymbol{\mu}) (\mathbf{x} - \boldsymbol{\mu})^T \boldsymbol{\Sigma}^{-1} p_{\mathbf{x}}(\mathbf{x}) d\mathbf{x}. \end{aligned} \quad (20)$$

Here, we denote  $(\mathbf{x} - \boldsymbol{\mu})^T \boldsymbol{\Sigma}^{-1} (\mathbf{x} - \boldsymbol{\mu})$  as  $t$ . We should also notice that  $(\boldsymbol{\Sigma}^{-1/2} (\mathbf{x} - \boldsymbol{\mu})) / \sqrt{t}$  has exactly the same distribution as  $\mathcal{S}$  in (1). We denote it as  $\mathbf{u}$  in the proof. More importantly, we can find that  $t$  is independent of  $\mathbf{u}$  because  $t = {}^d \mathcal{R}^2$  where  $\mathcal{R}$  is independent with  $\mathcal{S}$  in (1). Therefore, we have the following equations:

$$\begin{aligned} & \mathbb{E} \left[ \left( \frac{\partial \ln p_{\mathbf{x}}(\mathbf{x})}{\partial \boldsymbol{\mu}} \right) \cdot \left( \frac{\partial \ln p_{\mathbf{x}}(\mathbf{x})}{\partial \boldsymbol{\mu}} \right)^T \right] \\ &= 4 \int_{t, \mathbf{u}} \left( \frac{g'(t)}{g(t)} \right)^2 \cdot t \cdot \boldsymbol{\Sigma}^{-\frac{1}{2}} \mathbf{u} \mathbf{u}^T \boldsymbol{\Sigma}^{-\frac{1}{2}} p_{\mathbf{x}}(\mathbf{x}) d\mathbf{x} \\ &= 4 \int_t t \left( \frac{g'(t)}{g(t)} \right)^2 p_{\mathcal{R}^2}(t) dt \cdot \int_{\mathbf{u}} \boldsymbol{\Sigma}^{-\frac{1}{2}} \mathbf{u} \mathbf{u}^T \boldsymbol{\Sigma}^{-\frac{1}{2}} p_{\mathcal{S}}(\mathbf{u}) d\mathbf{u} \\ &= 4 \int_t t \left( \frac{g'(t)}{g(t)} \right)^2 p_{\mathcal{R}^2}(t) dt \cdot M^{-1} \boldsymbol{\Sigma}^{-1}. \end{aligned} \quad (21)$$

The last equation of (21) is obtained via  $\mathbb{E}[\mathbf{u} \mathbf{u}^T] = \frac{1}{M} \mathbf{I}$ . Thus, (3) is proved.

To calculate the Riemannian metric for the covariance matrix, we follow the work of [48] to calculate the Hessian of the Boltzman entropy of elliptical distributions. The Boltzman entropy is first obtained as follows,

$$\begin{aligned} H(\mathbf{x} | \boldsymbol{\Sigma}) &= \int_{\mathbf{x}} p_{\mathbf{x}}(\mathbf{x}) \ln p_{\mathbf{x}}(\mathbf{x}) d\mathbf{x} \\ &= \int_{\mathbf{x}} p_{\mathbf{x}}(\mathbf{x}) \left[ -\frac{1}{2} \ln |\boldsymbol{\Sigma}| + \ln c_M + \ln g(t) \right] d\mathbf{x} \\ &= -\frac{1}{2} \ln |\boldsymbol{\Sigma}| + \ln c_M + \int_{\mathbb{R}^M} p_{\mathcal{R}}(t) \ln g(t) dt. \end{aligned} \quad (22)$$

Because  $(\ln c_M + \int_{\mathbb{R}^M} p_{\mathcal{R}}(t) \ln g(t) dt)$  is irrelevant to  $\boldsymbol{\Sigma}$ , the Hessian of  $H(\mathbf{x} | \boldsymbol{\Sigma})$  can be calculated as

$$\frac{\partial H(\mathbf{x} | \boldsymbol{\Sigma} + s\boldsymbol{\Sigma}_0 + h\boldsymbol{\Sigma}_1)}{\partial s \partial h} \Big|_{s=0, h=0} = \frac{1}{2} \text{tr}(\boldsymbol{\Sigma}_0 \boldsymbol{\Sigma}^{-1} \boldsymbol{\Sigma}_1 \boldsymbol{\Sigma}^{-1}). \quad (23)$$

The Riemannian metric can thus be obtained as  $ds^2 = \frac{1}{2} \text{tr}(d\boldsymbol{\Sigma} \boldsymbol{\Sigma}^{-1} d\boldsymbol{\Sigma} \boldsymbol{\Sigma}^{-1})$ , which is the same as the case for multivariate normal distributions and is the mostly widely used metric.

This completes the proof of Lemma 1.

### B. Proof of Theorem 1

The proof of this property rests upon an expansion  $\mathbf{y}_n^T \tilde{\boldsymbol{\Sigma}}_k^{-1} \mathbf{y}_n$  to be  $(\mathbf{x}_n - \boldsymbol{\mu}_k)^T \boldsymbol{\Sigma}_k^{-1} (\mathbf{x}_n - \boldsymbol{\mu}_k) + \frac{1}{\lambda_k}$  in derivatives

of  $\tilde{J}$ . By setting  $\partial\tilde{J}/\partial\lambda_k = 0$  and  $\partial\tilde{J}/\partial c_k = 0$ , we then arrive at

$$\begin{aligned}\lambda_k &= -2 \frac{\sum_{n=1}^N \tilde{\xi}_{nk} \psi_k(t_{nk} + \frac{1}{\lambda_k} - c_k)}{\sum_{n=1}^N \tilde{\xi}_{nk}}, \\ c_k &= -\frac{1}{2} \frac{\sum_{n=1}^N \tilde{\xi}_{nk}}{\sum_{n=1}^N \tilde{\xi}_{nk} \psi_k(t_{nk} + \frac{1}{\lambda_k} - c_k)},\end{aligned}\quad (24)$$

where

$$\tilde{\xi}_{nk} = \frac{\pi_k \cdot c_M \cdot \sqrt{c_k \cdot \det(\tilde{\Sigma}_k^{-1})} \cdot g_k(\mathbf{y}_n^T \tilde{\Sigma}_k^{-1} \mathbf{y}_n - c_k)}{\sum_{k=1}^K \pi_k \cdot c_M \cdot \sqrt{c_k \cdot \det(\tilde{\Sigma}_k^{-1})} \cdot g_k(\mathbf{y}_n^T \tilde{\Sigma}_k^{-1} \mathbf{y}_n - c_k)}.\quad (25)$$

By inspecting  $\lambda_k = 1/c_k$ ,  $\det(\tilde{\Sigma}_k) = \lambda_k \cdot \det(\Sigma_k)$  and  $\mathbf{y}_n^T \tilde{\Sigma}_k^{-1} \mathbf{y}_n = (\mathbf{x}_n - \boldsymbol{\mu}_k)^T \Sigma_k^{-1} (\mathbf{x}_n - \boldsymbol{\mu}_k) + \frac{1}{\lambda_k}$ , we obtain  $\tilde{\xi}_{nk} = \xi_{nk}$  and  $\psi_k(t_{nk} + \frac{1}{\lambda_k} - c_k) = \psi_k(t_{nk})$ .

To prove the equivalence of the optimum of  $\tilde{\Sigma}_k$  in (10) and optima of  $\boldsymbol{\mu}_k$  and  $\Sigma_k$ , we directly calculate  $\partial\tilde{J}/\partial\tilde{\Sigma}_k$  in (10) and set it to 0, to yield

$$\tilde{\Sigma}_k = -2 \frac{\sum_{n=1}^N \tilde{\xi}_{nk} \psi_k(t_{nk} + \frac{1}{\lambda_k} - c_k) \mathbf{y}_n \mathbf{y}_n^T}{\sum_{n=1}^N \tilde{\xi}_{nk}}.\quad (26)$$

Again, as  $\lambda_k = 1/c_k$  and  $\tilde{\xi}_{nk} = \xi_{nk}$ , we arrive at

$$\begin{aligned}\tilde{\Sigma}_k &= -2 \frac{\sum_{n=1}^N \xi_{nk} \psi_k(t_{nk}) \mathbf{y}_n \mathbf{y}_n^T}{\sum_{n=1}^N \xi_{nk}} \\ &= -2 \frac{\sum_{n=1}^N \xi_{nk} \psi_k(t_{nk})}{\sum_{n=1}^N \xi_{nk}} \begin{bmatrix} \mathbf{x}_n \mathbf{x}_n^T & \mathbf{x}_n \\ \mathbf{x}_n^T & 1 \end{bmatrix}.\end{aligned}\quad (27)$$

By substituting  $\boldsymbol{\mu}_k$  and  $\Sigma_k$  of (8) and  $\lambda_k$  in (24), we then have the following equation

$$\tilde{\Sigma}_k = \begin{bmatrix} \Sigma_k + \lambda_k \boldsymbol{\mu}_k \boldsymbol{\mu}_k^T & \lambda_k \boldsymbol{\mu}_k \\ \lambda_k \boldsymbol{\mu}_k^T & \lambda_k \end{bmatrix},\quad (28)$$

which means that the optimum value  $\tilde{\Sigma}_k$  is exactly the reformulated form by the optimum values of (8).

This completes the proof of Theorem 1.

### C. Proof of Lemma 3

We here denote the contaminated distribution  $\mathcal{F} = (1 - \epsilon)\mathcal{F}_{\mathbf{x}} + \epsilon\mathcal{F}_{\mathbf{x}_0}$ , where  $\epsilon$  is the proportion of outliers;  $\mathcal{F}_{\mathbf{x}}$  is the true distribution of  $\mathbf{x}$  and  $\mathcal{F}_{\mathbf{x}_0}$  is the point-mass distribution at  $\mathbf{x}_0$ . For simplicity, we employ  $t$  to denote  $(\mathbf{x} - \boldsymbol{\mu}_j)^T \Sigma_j^{-1} (\mathbf{x} - \boldsymbol{\mu}_j)$  and  $t_0$  to denote  $(\mathbf{x}_0 - \boldsymbol{\mu}_j)^T \Sigma_j^{-1} (\mathbf{x}_0 - \boldsymbol{\mu}_j)$ . Then, the maximum log-likelihood estimation on the  $\Sigma_j$  of  $\mathcal{E}_j(\boldsymbol{\mu}_j, \Sigma_j, g_j)$  becomes

$$\begin{aligned}(1 - \epsilon) \mathbb{E}[\xi_j(\mathbf{x}) \psi_j(t) (\mathbf{x} - \boldsymbol{\mu}_j) (\mathbf{x} - \boldsymbol{\mu}_j)^T + \frac{1}{2} \xi_j(\mathbf{x}) \Sigma_j] \\ + \epsilon \xi_j(\mathbf{x}_0) \psi_j(t_0) (\mathbf{x}_0 - \boldsymbol{\mu}_j) (\mathbf{x}_0 - \boldsymbol{\mu}_j)^T + \epsilon \frac{\xi_j(\mathbf{x}_0)}{2} \Sigma_j = 0.\end{aligned}\quad (29)$$

We first calculate the IF (denoted by  $\mathcal{I}$  in the proof) when  $\Sigma_j = \mathbf{I}$  and  $\boldsymbol{\mu}_j = \mathbf{0}$ . Thus,  $t = \mathbf{x}^T \mathbf{x}$  and  $t_0 = \mathbf{x}_0^T \mathbf{x}_0$  in the following proof. Then, according to the definition of IF, we

differentiate (29) with respect to  $\epsilon$  and when it approaches 0, we arrive at

$$\begin{aligned}\mathbb{E}\left[\frac{\partial \xi_j(\mathbf{x})}{\partial \epsilon} \Big|_{\epsilon=0} \psi_j(t) \mathbf{x} \mathbf{x}^T\right] \\ + \xi_j(\mathbf{x}) \frac{\partial \psi_j(\mathbf{x}^T \Sigma_j^{-1} \mathbf{x})}{\partial \epsilon} \Big|_{\epsilon=0} \mathbf{x} \mathbf{x}^T + \frac{1}{2} \frac{\partial \xi_j(\mathbf{x})}{\partial \epsilon} \Big|_{\epsilon=0} \mathbf{I} + \frac{1}{2} \xi_j(\mathbf{x}) \mathcal{I} \\ + \xi_j(\mathbf{x}_0) \psi_j(t_0) \mathbf{x}_0 \mathbf{x}_0^T + \frac{1}{2} \xi_j(\mathbf{x}_0) \mathbf{I} = 0.\end{aligned}\quad (30)$$

In addition, we obtain

$$\begin{aligned}\frac{\partial \xi_j(\mathbf{x})}{\partial \epsilon} \Big|_{\epsilon=0} &= (\xi_j(\mathbf{x}) - \xi_j^2(\mathbf{x})) \cdot \left(-\frac{1}{2} \text{tr}(\mathcal{I}) - \psi_j(t) \mathbf{x}^T \mathcal{I} \mathbf{x}\right), \\ \frac{\partial \xi_j(\mathbf{x})}{\partial \epsilon} \Big|_{\epsilon=0} &= -\psi_j'(t) \mathbf{x}^T \mathcal{I} \mathbf{x}.\end{aligned}\quad (31)$$

By combining (30) and (31), we arrive at

$$\begin{aligned}\mathbb{E}\left[(\xi_j(\mathbf{x}) - \xi_j^2(\mathbf{x})) \cdot \left(-\frac{1}{2} \text{tr}(\mathcal{I}) - \psi_j(t) \mathbf{x}^T \mathcal{I} \mathbf{x}\right) \cdot (\psi_j(t) \mathbf{x} \mathbf{x}^T + \frac{1}{2} \mathbf{I})\right. \\ \left. - \xi_j(\mathbf{x}) \psi_j'(t) (\mathbf{x}^T \mathcal{I} \mathbf{x}) \mathbf{x} \mathbf{x}^T + \frac{1}{2} \xi_j(\mathbf{x}) \mathcal{I}\right] \\ + \xi_j(\mathbf{x}_0) \psi_j(t_0) \mathbf{x}_0 \mathbf{x}_0^T + \frac{1}{2} \xi_j(\mathbf{x}_0) \mathbf{I} = 0.\end{aligned}\quad (32)$$

It should be pointed out that  $(\mathbf{x} - \boldsymbol{\mu})^T \Sigma^{-1} (\mathbf{x} - \boldsymbol{\mu})$  has the same distribution as  $\mathcal{R}^2$ . It thus is independent of  $\frac{\Sigma^{-1/2}(\mathbf{x} - \boldsymbol{\mu})}{\sqrt{(\mathbf{x} - \boldsymbol{\mu})^T \Sigma^{-1} (\mathbf{x} - \boldsymbol{\mu})}}$  (denoted by  $\mathbf{u}$ ), which has the same distribution as  $\mathcal{S}$  (i.e., uniform distribution). For mixtures, when data are well-separated, those  $\mathbf{x}$  that does not belong to the  $j$ -th cluster has extremely low  $\xi_j(\mathbf{x})$ . In other words, the expectation in (32) is dominated by the expectation of the data which belong to the  $j$ -th cluster. Therefore, to calculate the expectation, we can treat the quadratic term  $(\mathbf{x} - \mathbf{0})^T \mathbf{I} (\mathbf{x} - \mathbf{0}) = \mathbf{x}^T \mathbf{x}$  (i.e.,  $t$ ) as independent of the normalised term  $\frac{\mathbf{I}^{-1/2}(\mathbf{x} - \mathbf{0})}{\sqrt{t}} = \frac{\mathbf{x}}{\sqrt{t}}$  (i.e.,  $\mathbf{u}$ ) of the  $j$ -th cluster.

Based on this approximation, we can rewrite (32) as

$$\begin{aligned}\mathbb{E}\left[(\xi_j(t) - \xi_j^2(t)) \cdot \left(-\frac{1}{2} \text{tr}(\mathcal{I}) - \psi_j(t) t \cdot \mathbf{u}^T \mathcal{I} \mathbf{u}\right) \cdot (\psi_j(t) t \cdot \mathbf{u} \mathbf{u}^T + \frac{1}{2} \mathbf{I})\right. \\ \left. - \xi_j(t) \psi_j'(t) t^2 (\mathbf{u}^T \mathcal{I} \mathbf{u}) \mathbf{u} \mathbf{u}^T + \frac{1}{2} \xi_j(t) \mathcal{I}\right] \\ + \xi_j(\mathbf{x}_0) \psi_j(t_0) \mathbf{x}_0 \mathbf{x}_0^T + \frac{1}{2} \xi_j(\mathbf{x}_0) \mathbf{I} = 0.\end{aligned}\quad (33)$$

Moreover, as  $\mathbf{u}$  is uniformly distributed, we have  $\mathbb{E}[\mathbf{u} \mathbf{u}^T] = \frac{1}{M} \mathbf{I}$ ,  $\mathbb{E}[\mathbf{u}^T \mathcal{I} \mathbf{u}] = \frac{1}{M} \text{tr}(\mathcal{I})$  and  $\mathbb{E}[(\mathbf{u}^T \mathcal{I} \mathbf{u}) \mathbf{u} \mathbf{u}^T] = \frac{1}{M(M+1)} (\mathcal{I} + \text{tr}(\mathcal{I}) \mathbf{I})$ . Thus, we arrive at

$$\begin{aligned}- \frac{(\mathbb{E}[(\xi_j(t) - \xi_j^2(t)) \psi_j^2(t) t^2] + \mathbb{E}[\xi_j(t) \psi_j'(t) t^2]) (\mathcal{I} + \text{tr}(\mathcal{I}) \mathbf{I})}{M(M+1)} \\ - \frac{1}{2M} \mathbb{E}[(\xi_j(t) - \xi_j^2(t)) \psi_j(t) t] \text{tr}(\mathcal{I}) \mathbf{I} - \frac{1}{4} \mathbb{E}[(\xi_j(t) - \xi_j^2(t))] \text{tr}(\mathcal{I}) \mathbf{I} \\ - \frac{1}{2M} \mathbb{E}[(\xi_j(t) - \xi_j^2(t)) \psi_j(t) t] \text{tr}(\mathcal{I}) \mathbf{I} + \frac{\pi_j}{2} \mathcal{I} \\ + \xi_j(\mathbf{x}_0) \psi_j(t_0) \mathbf{x}_0 \mathbf{x}_0^T + \frac{1}{2} \xi_j(\mathbf{x}_0) \mathbf{I} = 0.\end{aligned}\quad (34)$$

With  $w_1$  and  $w_2$  in (16), we can re-write (34) as

$$w_2 \mathcal{I} = w_1 \text{tr}(\mathcal{I}) \mathbf{I} - \xi_j(\mathbf{x}_0) \psi_j(t_0) \mathbf{x}_0 \mathbf{x}_0^T - \frac{1}{2} \xi_j(\mathbf{x}_0) \mathbf{I}.\quad (35)$$

Then, by taking trace on both sides of (35), we arrive at

$$\text{tr}(\mathcal{I}) = \frac{\xi_j(\mathbf{x}_0)\psi_j(t_0)\mathbf{x}_0\mathbf{x}_0^T + \frac{1}{2}\xi_j(\mathbf{x}_0)\mathbf{I}}{Mw_1 - w_2} \quad (36)$$

Thus, the IF at point  $\mathbf{x}_0$  of the  $j$ -th cluster, when  $\Sigma_j = \mathbf{I}$ , can be obtained as

$$\mathcal{I}(\mathbf{x}_0) = \left[ \frac{2w_1 \cdot \xi_j(\mathbf{x}_0)\psi_j(\mathbf{x}_0^T\mathbf{x}_0)\mathbf{x}_0^T\mathbf{x}_0 + w_2 \cdot \xi_j(\mathbf{x}_0)}{2(Mw_1 - w_2)w_2} \right] \cdot \mathbf{I} - \frac{\xi_j(\mathbf{x}_0)\psi_j(\mathbf{x}_0^T\mathbf{x}_0)}{w_2}\mathbf{x}_0\mathbf{x}_0^T. \quad (37)$$

The IF is then obtained at point  $\mathbf{x}_0$  of the  $j$ -th cluster for general  $\Sigma_j$  and  $\mu_j$  according to its affine equivalence (i.e.,  $\mathcal{I}_{\Sigma_j}(\mathbf{x}_0) = \Sigma_j^{1/2}\mathcal{I}(\Sigma_j^{-1/2}(\mathbf{x}_0 - \mu_j))\Sigma_j^{1/2}$ ).

This completes the proof of Lemma 3.

#### D. Proof of Lemma 4

Similar to the proof of Lemma 3, we have the following equation for estimating  $\mu_j$  with contaminated distribution  $\mathcal{F} = (1 - \epsilon)\mathcal{F}_{\mathbf{x}} + \epsilon\mathcal{F}_{\mathbf{x}_0}$ :

$$(1 - \epsilon)\mathbb{E}[\xi_j(\mathbf{x})\psi_j(t)\Sigma_j^{-1}(\mathbf{x} - \mu_j)] + \epsilon\xi_j(\mathbf{x}_0)\psi_j(t_0)\Sigma_j^{-1}(\mathbf{x}_0 - \mu_j) = 0 \quad (38)$$

Note that in (38), for simplicity we also use  $t$  to denote  $(\mathbf{x} - \mu_j)^T\Sigma_j^{-1}(\mathbf{x} - \mu_j)$  and  $t_0$  to denote  $(\mathbf{x}_0 - \mu_j)^T\Sigma_j^{-1}(\mathbf{x}_0 - \mu_j)$ . We here also utilise  $\mathcal{I}$  to denote the IF in this proof.

In addition, by differentiating with  $\epsilon$  and  $\epsilon \rightarrow 0$ , we arrive at

$$\mathbb{E}\left[\frac{\partial\xi_j(\mathbf{x})}{\partial\epsilon}\Big|_{\epsilon=0}\psi_j(t)\Sigma_j^{-1}(\mathbf{x} - \mu_j) + \xi_j(\mathbf{x})\frac{\partial\psi_j(t)}{\partial\epsilon}\Big|_{\epsilon=0}\Sigma_j^{-1}(\mathbf{x} - \mu_j) - \xi_j(\mathbf{x})\psi_j(t)\Sigma_j^{-1}\mathcal{I} + \xi_j(\mathbf{x}_0)\psi_j(t_0)\Sigma_j^{-1}(\mathbf{x}_0 - \mu_j)\right] = 0. \quad (39)$$

Besides, we also calculate

$$\begin{aligned} \frac{\partial\xi_j(\mathbf{x})}{\partial\epsilon}\Big|_{\epsilon=0} &= (\xi_j(\mathbf{x}) - \xi_j^2(\mathbf{x})) \cdot (-2\psi_j(t)(\mathbf{x} - \mu_j)^T\Sigma_j^{-1}\mathcal{I}) \\ \frac{\partial\psi_j(\mathbf{x})}{\partial\epsilon}\Big|_{\epsilon=0} &= -2\psi_j'(t)(\mathbf{x} - \mu_j)^T\Sigma_j^{-1}\mathcal{I}. \end{aligned} \quad (40)$$

When data are well separated, we can assume that  $t = (\mathbf{x} - \mu_j)^T\Sigma_j^{-1}(\mathbf{x} - \mu_j)$  is independent of  $\mathbf{u} = \frac{\Sigma_j^{-1/2}(\mathbf{x} - \mu_j)}{\sqrt{t}}$ . Therefore, (40) becomes

$$\begin{aligned} &2 \cdot \mathbb{E}[(\xi_j(\mathbf{x}) - \xi_j^2(\mathbf{x}))\psi_j^2(t)t] \cdot \mathbb{E}[\mathbf{u}^T\Sigma_j^{-\frac{1}{2}}\mathcal{I}\mathbf{u}] \\ &+ 2 \cdot \mathbb{E}[\xi_j(\mathbf{x})\psi_j'(t)t] \cdot \mathbb{E}[\mathbf{u}^T\Sigma_j^{-\frac{1}{2}}\mathcal{I}\mathbf{u}] + \mathbb{E}[\xi_j(\mathbf{x})\psi_j(t)]\Sigma_j^{-\frac{1}{2}}\mathcal{I} \\ &= \xi_j(\mathbf{x}_0)\psi_j(t_0)\Sigma_j^{-\frac{1}{2}}(\mathbf{x}_0 - \mu_j), \end{aligned} \quad (41)$$

which yields  $\mathbb{E}[\mathbf{u}^T\Sigma_j^{-\frac{1}{2}}\mathcal{I}\mathbf{u}] = \frac{1}{M}\Sigma_j^{-\frac{1}{2}}\mathcal{I}$ . Thus, we arrive at

$$\mathcal{I} = \frac{\xi_j(\mathbf{x}_0)\psi_j(t_0)(\mathbf{x}_0 - \mu_j)}{\frac{2}{M}\mathbb{E}[(\xi_j(\mathbf{x}) - \xi_j^2(\mathbf{x}))\psi_j^2(t)t] + \frac{2}{M}\mathbb{E}[\xi_j(\mathbf{x})\psi_j'(t)t] + \mathbb{E}[\xi_j(\mathbf{x})\psi_j(t)]}. \quad (42)$$

This completes the proof of Lemma 4.

## REFERENCES

- [1] M. A. T. Figueiredo and A. K. Jain, "Unsupervised learning of finite mixture models," *IEEE Transactions on Pattern Analysis and Machine Intelligence*, vol. 24, no. 3, pp. 381–396, 2002.
- [2] A. M. Zoubir, V. Koivunen, Y. Chakhchoukh, and M. Muma, "Robust estimation in signal processing: A tutorial-style treatment of fundamental concepts," *IEEE Signal Processing Magazine*, vol. 29, no. 4, pp. 61–80, 2012.
- [3] D. P. Mandic, D. Obradovic, A. Kuh, T. Adali, U. Trutschell, M. Golz, P. De Wilde, J. Barria, A. Constantinides, and J. Chambers, "Data fusion for modern engineering applications: An overview," in *Proceeding of International Conference on Artificial Neural Networks*. Springer, 2005, pp. 715–721.
- [4] K. W. Fang, S. Kotz, and K. W. Ng, *Symmetric multivariate and related distributions*. London, U.K.: Chapman & Hall, 1990.
- [5] P. J. Huber, "Robust statistics," in *International Encyclopedia of Statistical Science*. Springer, 2011, pp. 1248–1251.
- [6] H. Holzmann, A. Munk, and T. Gneiting, "Identifiability of finite mixtures of elliptical distributions," *Scandinavian Journal of Statistics*, vol. 33, no. 4, pp. 753–763, 2006.
- [7] D. Peel and G. J. McLachlan, "Robust mixture modelling using the t distribution," *Statistics and Computing*, vol. 10, no. 4, pp. 339–348, 2000.
- [8] J. L. Andrews and P. D. McNicholas, "Model-based clustering, classification, and discriminant analysis via mixtures of multivariate t-distributions," *Statistics and Computing*, vol. 22, no. 5, pp. 1021–1029, 2012.
- [9] T.-I. Lin, P. D. McNicholas, and H. J. Ho, "Capturing patterns via parsimonious t mixture models," *Statistics & Probability Letters*, vol. 88, pp. 80–87, 2014.
- [10] S. Tan and L. Jiao, "Multivariate statistical models for image denoising in the wavelet domain," *International Journal of Computer Vision*, vol. 75, no. 2, pp. 209–230, 2007.
- [11] R. P. Browne and P. D. McNicholas, "A mixture of generalized hyperbolic distributions," *Canadian Journal of Statistics*, vol. 43, no. 2, pp. 176–198, 2015.
- [12] J. T. Kent and D. E. Tyler, "Redescending M-estimates of multivariate location and scatter," *The Annals of Statistics*, pp. 2102–2119, 1991.
- [13] D. F. Andrews and C. L. Mallows, "Scale mixtures of normal distributions," *Journal of the Royal Statistical Society. Series B (Methodological)*, pp. 99–102, 1974.
- [14] T. Zhang, A. Wiesel, and M. S. Greco, "Multivariate generalized Gaussian distribution: Convexity and graphical models," *IEEE Transactions on Signal Processing*, vol. 61, no. 16, pp. 4141–4148, 2013.
- [15] S. Sra and R. Hosseini, "Geometric optimisation on positive definite matrices for elliptically contoured distributions," in *Advances in Neural Information Processing Systems*, 2013, pp. 2562–2570.
- [16] R. Hosseini and S. Sra, "Matrix manifold optimization for Gaussian mixtures," in *Advances in Neural Information Processing Systems*, 2015, pp. 910–918.
- [17] —, "An alternative to EM for Gaussian mixture models: Batch and stochastic riemannian optimization," *arXiv preprint arXiv:1706.03267*, 2017.
- [18] P.-A. Absil, R. Mahony, and R. Sepulchre, *Optimization algorithms on matrix manifolds*. Princeton University Press, 2009.
- [19] S. Bonnabel, "Stochastic gradient descent on Riemannian manifolds," *IEEE Transactions on Automatic Control*, vol. 58, no. 9, pp. 2217–2229, 2013.
- [20] Y. Liu, F. Shang, J. Cheng, H. Cheng, and L. Jiao, "Accelerated first-order methods for geodesically convex optimization on riemannian manifolds," in *Advances in Neural Information Processing Systems*, 2017, pp. 4868–4877.
- [21] H. Zhang, S. J. Reddi, and S. Sra, "Riemannian SVRG: Fast stochastic optimization on Riemannian manifolds," in *Advances in Neural Information Processing Systems*, 2016, pp. 4592–4600.
- [22] H. Zhang and S. Sra, "First-order methods for geodesically convex optimization," in *Proceeding of Conference on Learning Theory*, 2016, pp. 1617–1638.
- [23] S. J. Reddi, A. Hefny, S. Sra, B. Poczos, and A. Smola, "Stochastic variance reduction for nonconvex optimization," in *Proceeding of International Conference on Machine Learning*, 2016, pp. 314–323.
- [24] H. Zhang and S. Sra, "Towards Riemannian accelerated gradient methods," *arXiv preprint arXiv:1806.02812*, 2018.

- [25] C. RAO, "Information and accuracy attainable in the estimation of statistical parameters," *Bull. Calcutta Math. Soc.*, vol. 37, pp. 81–91, 1945.
- [26] L. T. Skovgaard, "A Riemannian geometry of the multivariate normal model," *Scandinavian Journal of Statistics*, pp. 211–223, 1984.
- [27] C. Atkinson and A. F. Mitchell, "Rao's distance measure," *Sankhyā: The Indian Journal of Statistics, Series A*, pp. 345–365, 1981.
- [28] S.-I. Amari, "Differential geometry of curved exponential families—curvatures and information loss," *The Annals of Statistics*, pp. 357–385, 1982.
- [29] —, "Natural gradient works efficiently in learning," *Neural Computation*, vol. 10, no. 2, pp. 251–276, 1998.
- [30] S. Cambanis, S. Huang, and G. Simons, "On the theory of elliptically contoured distributions," *Journal of Multivariate Analysis*, vol. 11, no. 3, pp. 368–385, 1981.
- [31] G. Frahm, "Generalized elliptical distributions: Theory and applications," Ph.D. dissertation, Universität zu Köln, 2004.
- [32] O. Arslan, "Convergence behavior of an iterative reweighting algorithm to compute multivariate M-estimates for location and scatter," *Journal of Statistical Planning and Inference*, vol. 118, no. 1-2, pp. 115–128, 2004.
- [33] B. G. Lindsay, "Mixture models: Theory, geometry and applications," in *NSF-CBMS Regional Conference Series in Probability and Statistics*. JSTOR, 1995, pp. i–163.
- [34] J. Sun, A. Kaban, and J. M. Garibaldi, "Robust mixture modeling using the Pearson type VII distribution," in *Proceeding of The IEEE International Joint Conference on Neural Networks (IJCNN)*. IEEE, 2010, pp. 1–7.
- [35] A. Wiesel, "Geodesic convexity and covariance estimation," *IEEE Transactions on Signal Processing*, vol. 60, no. 12, pp. 6182–6189, 2012.
- [36] D. Karlis and L. Meligkotsidou, "Finite mixtures of multivariate Poisson distributions with application," *Journal of Statistical Planning and Inference*, vol. 137, no. 6, pp. 1942–1960, 2007.
- [37] E. López-Rubio, "Stochastic approximation learning for mixtures of multivariate elliptical distributions," *Neurocomputing*, vol. 74, no. 17, pp. 2972–2984, 2011.
- [38] R. P. Browne, P. D. McNicholas, and M. D. Sparling, "Model-based learning using a mixture of mixtures of Gaussian and uniform distributions," *IEEE Transactions on Pattern Analysis and Machine Intelligence*, vol. 34, no. 4, pp. 814–817, 2012.
- [39] R. A. Redner and H. F. Walker, "Mixture densities, maximum likelihood and the em algorithm," *SIAM Review*, vol. 26, no. 2, pp. 195–239, 1984.
- [40] M. I. Jordan and R. A. Jacobs, "Hierarchical mixtures of experts and the EM algorithm," *Neural Computation*, vol. 6, no. 2, pp. 181–214, 1994.
- [41] I. Naim and D. Gildea, "Convergence of the EM algorithm for gaussian mixtures with unbalanced mixing coefficients," *arXiv preprint arXiv:1206.6427*, 2012.
- [42] R. Salakhutdinov, S. T. Roweis, and Z. Ghahramani, "Optimization with EM and expectation-conjugate-gradient," in *Proceedings of the 20th International Conference on Machine Learning (ICML-03)*, 2003, pp. 672–679.
- [43] B. Jeuris, R. Vandebril, and B. Vandereycken, "A survey and comparison of contemporary algorithms for computing the matrix geometric mean," *Electronic Transactions on Numerical Analysis*, vol. 39, no. EPFL-ARTICLE-197637, pp. 379–402, 2012.
- [44] S. Sra, "A new metric on the manifold of kernel matrices with application to matrix geometric means," in *Advances in Neural Information Processing Systems*, 2012, pp. 144–152.
- [45] S. Jayasumana, R. Hartley, M. Salzmann, H. Li, and M. Harandi, "Kernel methods on the Riemannian manifold of symmetric positive definite matrices," in *Proceeding of The IEEE Conference on Computer Vision and Pattern Recognition*. IEEE, 2013, pp. 73–80.
- [46] M. Faraki, M. T. Harandi, and F. Porikli, "A comprehensive look at coding techniques on Riemannian manifolds," *IEEE Transactions on Neural Networks and Learning Systems*, 2018.
- [47] J. Burbea and C. R. Rao, "Entropy differential metric, distance and divergence measures in probability spaces: A unified approach," *Journal of Multivariate Analysis*, vol. 12, no. 4, pp. 575–596, 1982.
- [48] F. Hiai and D. Petz, "Riemannian metrics on positive definite matrices related to means," *Linear Algebra and its Applications*, vol. 430, no. 11-12, pp. 3105–3130, 2009.
- [49] M. Calvo and J. M. Oller, "A distance between multivariate normal distributions based in an embedding into the Siegel group," *Journal of Multivariate Analysis*, vol. 35, no. 2, pp. 223–242, 1990.
- [50] C. Jin, Y. Zhang, S. Balakrishnan, M. J. Wainwright, and M. I. Jordan, "Local maxima in the likelihood of Gaussian mixture models: Structural results and algorithmic consequences," in *Advances in Neural Information Processing Systems*, 2016, pp. 4116–4124.
- [51] N. Boumal and P.-A. Absil, "Low-rank matrix completion via preconditioned optimization on the Grassmann manifold," *Linear Algebra and its Applications*, vol. 475, pp. 200–239, 2015.
- [52] E. Ollila and D. E. Tyler, "Regularized M-estimators of scatter matrix," *IEEE Transactions on Signal Processing*, vol. 62, no. 22, pp. 6059–6070, 2014.
- [53] R. A. Maronna, "Robust M-estimators of multivariate location and scatter," *The Annals of Statistics*, pp. 51–67, 1976.
- [54] D. E. Tyler, "Breakdown properties of the M-estimators of multivariate scatter," *arXiv preprint arXiv:1406.4904*, 2014.
- [55] E. Ollila, D. E. Tyler, V. Koivunen, and H. V. Poor, "Complex elliptically symmetric distributions: Survey, new results and applications," *IEEE Transactions on Signal Processing*, vol. 60, no. 11, pp. 5597–5625, 2012.
- [56] F. R. Hampel, E. M. Ronchetti, P. J. Rousseeuw, and W. A. Stahel, *Robust statistics: the approach based on influence functions*. John Wiley & Sons, 2011, vol. 196.
- [57] C. Hennig *et al.*, "Breakdown points for maximum likelihood estimators of location–scale mixtures," *The Annals of Statistics*, vol. 32, no. 4, pp. 1313–1340, 2004.
- [58] N. Boumal, B. Mishra, P.-A. Absil, and R. Sepulchre, "Manopt, a Matlab toolbox for optimization on manifolds," *Journal of Machine Learning Research*, vol. 15, pp. 1455–1459, 2014. [Online]. Available: <http://www.manopt.org>
- [59] S. Dasgupta, "Learning mixtures of gaussians," in *40th Annual Symposium on Foundations of Computer Science*. IEEE, 1999, pp. 634–644.
- [60] P. Arbelaez, M. Maire, C. Fowlkes, and J. Malik, "Contour detection and hierarchical image segmentation," *IEEE Trans. Pattern Anal. Mach. Intell.*, vol. 33, no. 5, pp. 898–916, May 2011. [Online]. Available: <http://dx.doi.org/10.1109/TPAMI.2010.161>
- [61] A. Vedaldi and B. Fulkerson, "VLFeat: An open and portable library of computer vision algorithms," <http://www.vlfeat.org/>, 2008.
- [62] Z. Wang, A. C. Bovik, H. R. Sheikh, E. P. Simoncelli *et al.*, "Image quality assessment: From error visibility to structural similarity," *IEEE Transactions on Image Processing*, vol. 13, no. 4, pp. 600–612, 2004.
- [63] A. E. Mitchell, "The information matrix, skewness tensor and a-connections for the general multivariate elliptic distribution," *Annals of the Institute of Statistical Mathematics*, vol. 41, no. 2, pp. 289–304, 1989.